原 著

Infantile neuroaxonal dystrophyの早期診断に関する検討*

塩田 睦記[1)], 宍倉 啓子[1)], 吉井 啓介[1)], 児玉 美帆[1)]
松尾 真理[1)], 佐々木香織[1)], 田良島美佳子[1)], 舟塚 真[1)]
鈴木 暢子[1)], 小国 弘量[1)], 大澤真木子[1)], 原 正道[2)]

要旨：Infantile neuroaxonal dystrophy (INAD) は乳児期後半に発症し、運動・知能障害を呈する常染色体劣性遺伝疾患である。我々は皮膚生検で確定診断し得た典型的2症例を経験し、早期診断に有用と考えられる共通の臨床及び検査所見をretrospectiveに検討した。その結果、①退行以前からの血清asparate aminotransferase(AST), lactate dehydrogenase(LDH)軽度上昇、②creatin kinase (CK) 高値を伴わない著明な筋緊張低下、③頭部MRIでの小脳の萎縮とT2強調画像での高信号、④脳波での全般性高振幅速波、⑤末梢運動神経伝導速度は正常、の所見が注目された。特に①と③の組み合わせは特徴的な検査所見であり、本症の早期診断に有用と考えられた。また、病理学的に小脳の病変が早期から顕著である点に考察を加えた。

Key Words: 乳児型神経軸索ジストロフィー, 小脳萎縮, グリオーシス, ジストロフィー様軸索, MRI画像

末梢神経 2004; 15(1): 71–78

はじめに

Infantile neuroaxonal dystrophy (INAD) は1952年にSeitelbergerが初めて報告し[1)]、1963年にCowenとOlmsteadによって命名された常染色体劣性遺伝疾患である[2)]。臨床的には6ヶ月から2歳までの乳児期後半より急激に発症し、進行性の運動知能障害を呈し、10歳前後で死亡することが多い。確定診断は、中枢・末梢神経にdystrophic axonを確認することでなされる[3)]。しかし発症病態はいまだ不明であり、特異的な臨床所見や検査値がなく、発病初期にINADを疑うことはしばしば困難である。我々は、最近典型的2症例を経験し、本症の早期診断の留意点につきretrospectiveに検討した結果、生化学検査と頭部MRI所見が有用であると結論したので報告する。また、中枢神経系の病理学的所見と特徴的な頭部MRI所見との関連性につき比較検討したのであわせて報告する。

症 例

症例1 3歳0ヶ月女児

【初発症状】1歳6ヶ月 精神運動発達遅滞

【家族歴】同胞の姉5歳は健康。父方伯母幼少期に死亡。

---

* Early diagnostic points in infantile neuroaxonal dystrophy

[1)]Mutsuki SHIODA, M.D., Keiko SHISHIKURA, M.D., Keisuke YOSHII, M.D., Miho KODAMA, M.D., Mari MATSUO, M.D., Kaori SASAKI, M.D., Mikako TARASHIMA, M.D., Makoto FUNATSUKA, M.D., Haruko SUZUKI, M.D., Hirokazu OGUNI, M.D., Makiko OSAWA, M.D.：東京女子医科大学小児科〔〒161-8666 東京都新宿区河田町8-1〕; Division of Neurology, Department of Pediatrics School of Medicine Tokyo Women's Medical University, Tokyo

[2)]Masamichi HARA, M.D.：横浜市立大学医学部付属病院〔〒236-0004 横浜市金沢区福浦3-9〕; Yokohama City University, School of Medicine, Yokohama

父方従姉（9歳）は脳性麻痺に、従妹（7歳）はてんかんに罹患。

【既往歴】妊娠中特記すべき合併症なし。

在胎37週、体重2910 g、頭位自然分娩。

【発達歴】定頸3ヶ月，坐位6ヶ月，つたい歩き9ヶ月。

有意語1歳。

【現病歴】生後3ヶ月に海外移住のため行った血液検査でAST高値を指摘された。その後も定期的に血液検査を施行したが同様であった。健診では特に異常を指摘されなかった。1歳になっても独歩なく、言葉も増えず、1歳6ヶ月時他院で精査をした。AST, LDH軽度高値であったため筋疾患が疑われ、2歳時に頭部CT，頭部MRI、脳波検査を施行されたが、異常は認められなかった。この頃から右優位の内斜視を認めた。2歳6ヶ月には筋生検が施行されたが、異常は認められなかった。その直後から精神・運動発達の退行が出現し、2歳7ヶ月に伝い歩きをしなくなった。言葉も減少し、眼振が出現した。2歳10ヶ月になって足関節が尖足位で拘縮し、2歳11ヶ月から這い這いをしなくなった。3歳時、座位のみとなったため当科での精査を希望し入院した。

【入院時現症】

座位はとんび座り。うつぶせから座位可能。寝返りは側臥位まで可能。筋緊張は著明に低下(double folding, window徴候, scarf徴候, loose shoulder陽性)。固視・追視あり。水平方向の注視眼振を認める。右優位の内斜視あり。胸腹部異常所見なし。肝脾腫なし。上下肢深部腱反射亢進、Babinski反射陽性で下肢に痙性を認めた。足関節尖足位で内反し、背屈制限あり。測定障害あり。眼底では視神経乳頭の蒼白を認めた。

【検査所見】

血液検査所見では、血清AST、LDHの軽度高値（AST 118I/U, LDH 462I/U：分画1,2上昇、5低下）を認めたが、CKは正常（CK 94U/I）であり、乳酸、ピルビン酸は正常上限（乳酸18.6mg/dl, ピルビン酸1.05mg/dl）であった。白血球ライソゾーム、有機酸分析に異常を認めなかった。α-N-acetylgalactosaminidaseも正常であり、Schindler病は否定された。また、髄液でもLDH, 77I/U（30I/U以下）の軽度高値を認めた。

電気生理学的所見では、脳波の全般性高振幅速波、視覚誘発電位（VEP）の波形分離不良を認めた。聴性脳幹反応（ABR)、脛骨神経の運動神経伝導速度（MCV）は正常であった。

頭部MRI（図1）：T1強調画像矢状断では、小脳の著明な萎縮を認めた。T2強調画像冠状断では、Flair画像がないため脳脊髄液との区別が難しいが、小脳皮質の高信号を認めた。T2強調画像水平断では、小脳の萎縮は認められたが、小脳皮質の高信号は明らかではなかった。1歳11ヶ月時の退行以前に他院で施行された頭部MRIでは、T2強調画像での小脳皮質高信号は見出されなかったが、小脳の萎縮はすでに認められた。

皮膚生検：腋窩部の皮膚の組織病理学的検査を施行した。電子顕微鏡低倍率像（図2）では、正常の軸索とともに、多数のdystrophic axonを汗腺周辺の末梢神経終末に認めた。高倍率像では、軸索内の膜様管状構造物を認めた。

以上の臨床経過、検査所見よりINADと確定診断された。

症例2　1歳11ヶ月女児

【初発症状】9ヶ月　筋緊張低下

【家族歴】神経筋疾患なし．近親婚なし．母親の流産歴なし．

【既往歴】切迫早産のため妊娠7ヶ月より母親は投薬を受けていた。

在胎39週、体重3160g、吸引分娩。

1歳3ヶ月と1歳6ヶ月時にチアノーゼを伴う20～30秒ほどの泣き入りひきつけがみられた。

【発達歴】定頸3ヶ月，寝返り6ヶ月，坐位8ヶ月，いざり這い1歳、這い這い1歳6ヶ月喃語1歳6月

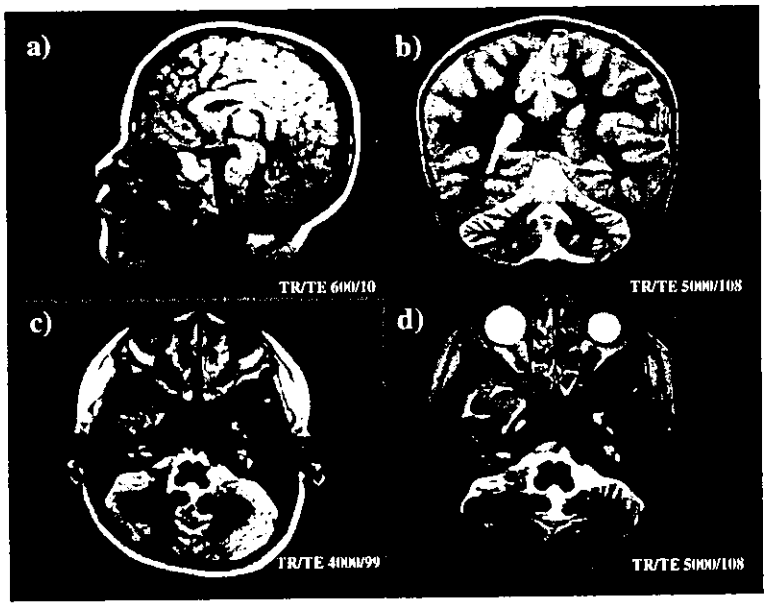

図1 a) 3歳0ヶ月T1強調画像矢状断で小脳の著明な萎縮を認める。
b) 3歳0ヶ月T2強調画像冠状断で小脳皮質の高信号を認める。
c) 1歳11ヶ月退行以前のT2強調画像水平断でも小脳皮質の萎縮を認める。
d) 3歳0ヶ月T2強調画像水平断では小脳萎縮を認めるが、小脳の高信号は明らかではない。

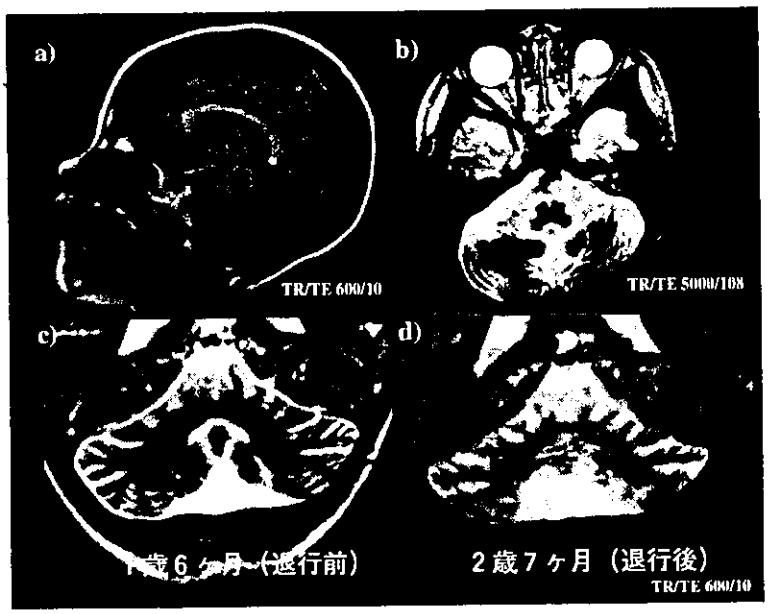

図2 a) 1歳11ヶ月T1強調画像矢状断で小脳の著明な萎縮を認める。
b) 1歳11ヶ月T2強調画像水平断で小脳の萎縮を認める。
c) 1歳6ヶ月退行以前のT2強調画像冠状断では小脳皮質の高信号を認める。
d) 2歳7ヶ月退行後のT2強調画像冠状断では小脳皮質の高信号を認める。

【現病歴】生後9カ月頃より体がやわらかいことに母親は気づいていたが、健診などで指摘されたことはなかった。1歳になっても独歩なく発達遅延を指摘された。1歳6ヶ月某病院にて、血液・脳波・頭部MRI等の精査を受けるが、ASTの軽度高値ほか異常を指摘されなかった。1歳7ヶ月39.0度の発熱があり、解熱剤により1日で解熱したが、この日より座位保持・寝返り・定頚ができなくなった。表情は乏しくなり、喃語も認められなくなった。1歳9ヶ月より眼振を認めるようになったため、1歳11ヶ月時精査目的で入院した。

【入院時現症】

仰臥位姿勢ではfrog postureをとり、表情は乏しかった。喃語なく発語のみ。定頚不可能であったが、上肢の抗重力運動可。筋緊張は著明に低下（double folding, window徴候, scarf徴候, loose shoulder陽性）。固視・追視あり。水平方向の注視眼振あり。胸腹部異常所見なし。肝脾腫なし。上肢深部腱反射正常。膝蓋腱反射亢進。アキレス腱反射消失。Babinski反射陽性。測定障害あり。眼底では視神経乳頭の蒼白を認めた。

【検査所見】

血液検査所見では、血清AST、LDHの軽度高値（AST 108I/U. LDH 459U/I）を認めた。CKは正常（CK 48U/I）であり、乳酸、ピルビン酸は正常上限（乳酸17.2mg/dl. ピルビン酸0.80mg/dl）であった。白血球ライソゾーム、有機酸分析、α-N-acetylgalactosaminidaseは正常であった。

電気生理学的所見では、脳波の全般性高振幅速波、VEPの波形分離不良を認めた。ABR、正中神経、脛骨神経のMCV、正中神経、腓骨神経の知覚神経伝導速度（SCV）は正常であった。針筋電図所見では、脱神経所見が認められた。

頭部MRI（図3）：1歳11ヵ月の頭部MRIでは著明な小脳の萎縮を認めた。2歳7ヶ月時の頭部MRIT2強調画像冠状断では小脳皮質の高信号が認められた。1歳6ヶ月の頭部MRI冠状断でも小脳の萎縮と小脳皮質の高信号が認められた。

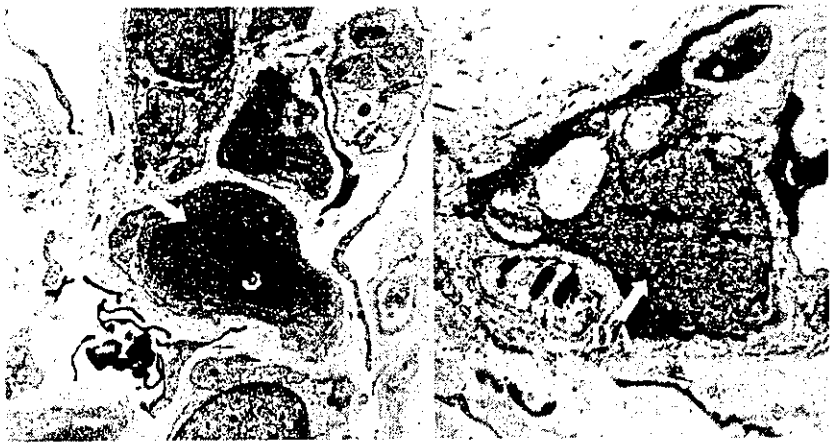

図3 汗腺の電気顕微鏡学的所見
症例1の低倍像（×6000）では多数のDAを認めた。
症例2の高倍像（×15000）では軸索内の膜様管状構造物を認めた。

皮膚生検：腋窩部の皮膚の組織病理学的検査を施行した。電子顕微鏡にて軸索内の膜様管状構造物を認めた。

以上の臨床経過、検査所見よりINADと確定診断された。

考　察

表1に2症例の臨床像のまとめを示す。2症例とも2歳前後にはじまる急激な退行を示した。神経学的所見では、著明な筋緊張低下、眼振、測定障害、深部腱反射の亢進、Babinski反射陽性等の錐体路症状、視神経乳頭の蒼白が認められた。また、両症において汗腺周囲の末梢神経にいわゆるdystrophic axonが認められINADの確定診断が行われた。錐体外路症状、知覚障害、けいれんは認められなかった。症例2では、アキレス腱反射が消失し、末梢神経障害が存在すると判断した。

表2に2症例に共通する検査所見を示す。

INADは乳児期後期より急激な退行で発症するが、退行以前にもAST、LDHの軽度高値、筋緊張低下、頭部MRIでの小脳の萎縮は注目すべき所見であり、本症の発症は退行が認められる以前であると考えられた。症例2では1歳までの発達はほぼ正常であったが、その時点ですでにASTの軽度高値を指摘されていた。INADの発症病態は未だに不明であるが、AST, LDHの上昇は神経性の変性あるいは神経細胞の軸索輸送に関与する何らかの酵素異常を意味すると考えられている[4]。過去の症例報告でも血清AST, LDHの軽度高値は報告されているが、AST, LDHの上昇は特異的所見ではないため、あまり注目されてこなかった。しかし、退行の発症年齢、CK高値を伴わない著明な筋緊張低下、錐体路徴候などの臨床症状と合わせれば、INADの早期診断に有用な所見と思われる。また、本症が常染色体劣性遺伝疾患であることから、同胞罹患の有無の早期診断に、血清AST軽

表1

	症例1（女児）	症例2（女児）
初診時年齢	3歳0ヶ月	1歳11ヶ月
初発症状（年齢）	精神・運動発達遅滞（1歳6ヶ月）	筋緊張低下（9ヶ月）
初診時発達レベル	座位 喃語のみ	定頚不可 喃語なし
最高発達レベル	伝い歩き（9ヶ月） 有意語（1歳）	這い這い（1歳6ヶ月） 喃語（1歳6ヶ月）
退行出現年齢	2歳7ヶ月	1歳7ヶ月
現在の運動レベル	支持座位（3歳6ヶ月）	寝たきり（2歳9ヶ月）

表2　2症例に共通する検査所見

血液生化学など	症例1：AST 118↑ LDH 462↑（髄液でも軽度上昇） 症例2：AST 108↑ LDH 459↑（髄液で検査なし） 白血球ライソゾーム酵素 α-Nacetylgalactosaminidase 正常 血清、髄液中の乳酸、ピルビン酸の著明な上昇はなし
電気生理学的検査（初診時）	ABR・SCV・MCV 正常 VEP：波形分離不良 EMG：脱神経所見（症例2のみ） 脳波：全般性高振幅性速波を認める

度高値は有用であると推定される。

また、頭部MRIでは非常に特徴的な所見が得られた。T1強調画像矢状断では、小脳の著明な萎縮が明らかであった[5]。T2強調画像冠状断では、小脳皮質の高信号を認められたが、脳脊髄液との区別のためFlair画像を同時に行うことが必要と思われた。一方、T2強調画像水平断では、小脳の萎縮を認めるが、小脳皮質の高信号は明らかではなった。INADで時に認められるT2強調画像での淡蒼球・黒質・大脳白質の低信号は認められなかった[6),7)]。また、2症例とも退行以前に頭部MRIを施行しており、T2強調画像冠状断では、小脳皮質の萎縮と皮質の高信号を認めたが、水平断では、萎縮のみ認めた。小児の代謝・変性疾患の多くは小脳に病変があるにもかかわらず、MRI画像上ではINADで認めるような異常信号を小脳に認めず、本所見はINADに特異的な所見といえる。

BarlowらはINADの発症7ヶ月の症例でもすでに小脳のT2高信号を認めることを報告しており[8)]、INADでは小脳が最も早期から重度に変性すると推測していた。臨床的に小脳症状は著明であり、2症例とも退行が出現する前から頭部MRIで、萎縮・皮質の高信号と特徴的な所見を認めたことから、本症における小脳症状の重要性が示唆された。一方、過去の剖検例の報告によると、小脳ではINADに特徴的なspheroid bodyは散在、もしくはほとんど認められなかったとするものが多い[9),10),11)]。共著者原による神奈川こども医療センターの剖検例の検討では、小脳皮質の病理学的所見は著明なプルキンエ細胞と顆粒細胞の脱落、グリオーシスであり、その程度は剖検時の年齢とは相関せず、低年齢児でも非常に著明なグリオーシスを認めた。また、spheroid bobyはごくわずかに認められるにすぎなかった。これは小脳の病変が早期から非常に強いため、神経細胞の変性、脱落がすでに高度に進行していたため、dystrophic axonも見出せなくなった可能性が示唆された。頭部MRIでの小脳萎縮・皮質の高信号はこのグリオーシスを反映していると考えられた。また、この所見を得るには冠状断が有用であったが、脳脊髄液との鑑別のため、Flair画像での比較検討が今後強く望まれる。

INADの病因は未だ不明であり、治療法も認められていない。組織所見の特徴のひとつとなるspheroidはINADに特徴的な所見ではない。ビタミンE欠乏にでもaxonの腫大が起こる。本症でのビタミンEの定量では対照との有意な差を認めず、血中ビタミンEを高値に維持しても臨床的には明らかな機能の改善はみられなったと報告されている[12)]。両症例にはビタミンB1,B2,Eを投与して、表情が豊かになったと臨床的な改善を認めたが、定量的な評価は未施行であり、今後検討する予定である。

まとめ

INAD2症例の臨床及び検査所見から、退行以前の血清AST,LDHの軽度上昇、筋緊張の低下、頭部MRIでの小脳萎縮とT2強調画像での小脳皮質の高信号が本症に特徴的な所見として注目された。T2強調画像での小脳皮質の高信号が、水平断では明らかではなく、冠状断が最も有用であったが、確定にはFlair画像での比較検討が望まれた。また、病理学的にも、小脳の病変は早期から顕著であると推察された。

謝　辞

中枢神経系の病理所見についてご指導をいただいた神奈川こども医療センター神経内科山下純正先生、また、α-N-acetylgalactosaminidaseの測定をしていただきました鹿児島大学医学部付属病院皮膚科神田彰先生に深謝いたします。

引用文献

1) Seitelberger F: Eine unbekannte Form von infantiler lipoid-speicher Krankheit des Gehirns. In: Proceedings of First International Congress of Neuropathology, vol.3, Turin: Rosenberg and Sellier, pp323-333, 1952
2) Cowen D, Olmstead EV: Infantile neuroaxonal

dystrophy. *J Neuropathol Exp Neurol* 22: 175-236, 1963
3) 木村清次、岩本弘子、佐々木佳郎、ほか:Infantile neuroaxonal dystrophyの末梢神経所見. *脳と発達* 18: 8-13, 1986
4) 小林康子:Infantile neuroaxonal dystrophy. 小児内科28増刊号: 760-762, 1996
5) 石井光子、田辺雄三、後藤実千代、ほか:MRIが診断に有用であったinfantile neuroaxonal dystrophyの1例. *脳と発達* 24: 491-493, 1992
6) Nardocci N, Zorzi G, Farina L, *et al.*: Infantile neuroaxonal dystrophy. Clinical spectrum and diagnostic criteria: *Neurology* 52: 1472-1478, 1999
7) Farina L, Nardocci N, Bruzzone MG, *et al.*: Infantile neuroaxonal dystrophy: neuroradiological studies in 11 patients. *Neuroradiology* 41: 376-380, 1999
8) Barlow JK, Sims KB, Kolodny EH: Early cerebellar degeneration in twins with infantile neuroaxonal dystrophy. *Ann Neurol* 25: 413-415, 1989
9) 山下純正、山田美智子、岩本弘子、ほか:Infantile neruoaxonal dystrophyにおける小脳の神経病理学的検討. 第39回日本神経病理学会, 1998
10) Tanabe Y, Iai M, Ishii M, *et al.*: The use of magnetic resonance imaging in diagnosing infantile neuroaxonal dystrophy. *Neurology* 43: 110-113, 1993
11) 伊東恭子、河合神二、西野昌光、ほか:発症初期より経過を追えたinfantile neruoaxonal dystrophyの兄弟例—臨床増像、画像診断、電気生理学的、病理学的所見について. *脳と発達* 24: 283-288, 1992
12) 湯浅洸、横田清、満留昭久、ほか:Infantile neuroaxonal dystrophyの同胞例. *脳と発達* 5: 182-190, 1973

研究 臨床

第66回学術講演会(4)

小児の意識障害のみかた
— Reye 症候群の剖検例より学ぶこと—

東京女子医科大学小児科 近田照己、舟塚 真、斎藤加代子、大澤真木子

1 はじめに

意識障害に陥る原因、疾患は多岐にわたり、臨床の場面では迅速かつ正確な鑑別診断と治療が要求される。成人では外傷以外には脳血管障害の頻度が高いが、小児では感染症、代謝異常症、薬物中毒、痙攣性疾患などが重要である。今回、喘息様気管支炎後にReye症候群を発症し、基礎疾患として脂肪酸代謝異常症が疑われた1剖検例を経験した。テオフィリン製剤の関与も否定できない。症例を提示し、問題点を検討した。また、小児の意識障害のみかたのポイントを概説した。

2 症例提示

(1) 症例

症例は3歳女児。健康な1歳の妹がいる。成長・発達に特に問題なし。気管支喘息、痙攣の既往なし。

(2) 現病歴

平成14年5月11日より喘息様気管支炎を発症し、テオフィリン製剤と鎮咳薬他（詳細不明）の内服をしていた。翌日発熱したが、解熱剤の内服はしていなかった。5月13日、7～8回の嘔吐があったが、意識は清明だった。14日16時49分、全身性強直性間代痙攣があり、他院にてジアゼパム、フェノバルビタール等使用したが、痙攣は消失せず、当院搬送となった。

(3) 入院時現症

体温41℃、意識レベルはJCS300で痛み刺激への反応はなし。また、瞳孔径は2～3㎜で、左右差はなく、対光反射は消失していた。口唇は乾燥。項部硬直はなし。頻拍、多呼吸、喘鳴、呼気延長を認めた。腹部は平坦で、ツルゴール低下。肝臓を1㎝触知、脾臓は触知しなかった。皮膚所見なし。浮腫なし。深部腱反射は消失していた。

(4) 入院時検査所見

血算：WBC 10800/μl（好中球47%、リンパ球51%）、Hb 11.0g/dl、Plt 24.5万/μl。

凝固系：PT 13.5秒、APTT 50.3秒、Dダイマー 5.04μg/ml、TAT 41.4ng/ml。

生化学：AST 140IU/l、ALT 48IU/l、LDH 976IU/l、BUN 16.9mg/dl、Cr 7.2mg/dl、Na 121mEq/l、Cl 89mEq/l、Ca 7.2mWq/l、K 6.7mEq/l, CRP 1.09mg/dl、CK 273IU/l、尿酸 14.5mg/dl、NH3 147 μg/dl、血糖 258mg/dl。

血液ガス分析（挿管、酸素投与下）：pH 7.317、PC02 28.3㎜Hg、P02 133.2㎜Hg、BE -9.5㎜ol/l、HCO3- 14.6㎜Hg。

Theophylline濃度： 12.04 μg/ml。

検尿：蛋白(1+)、糖(−)、潜血(−)、ケトン(3+)。

頭部CT：出血、梗塞はなし。明らかな浮腫もなし。

胸部Xp：CTR49%。明らかな肺炎像なし。

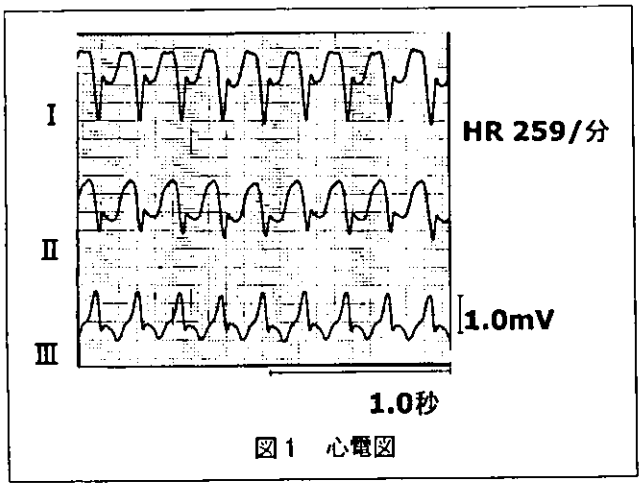

図1　心電図

心電図：心拍数毎分259回、心室頻拍の所見。【図1】

（5）入院後の検査所見の推移【図2】

AST、ALT、LDH、CKの急速な上昇が認められた。血糖は、入院時258mg/dlと高血糖であったが、その後、痙攣があったため、血糖測定したところ3.2%糖含有の補液を継続していたにも拘らず17mg/dlと低血糖を呈していた。グルコース静注後低血糖は補正された。アンモニアは軽度高値のままであった。血液ガスでは、乳酸値の上昇に伴う代謝性アシドーシスの高度な進行が認められた。

（6）入院後経過

入院時、痙攣は約1時間10分持続していたが、チオペンタール100mg静注にておさまった。呼吸困難に対し、気管内挿管、酸素投与を行い、同時に、鎮静、痙攣予防のため、ミダゾラム0.2mg/kg/時の持続静注を開始した。アシドーシス補正のため重炭酸ナトリウム静注を、脳浮腫対策として、グリセオール点滴を施行した。19時20分、心室頻拍があり除細動を施行した。当初、テオフィリン関連痙攣を疑いテオフィリン血中濃度を測定したが、12.04μg/dlとやや高めながらも治療域だった。多呼吸、呼気延長、喘鳴を認め、20時より人工呼吸器管理、プレドニゾロン静注、アミノフィリン0.5mg/kg/時持続点滴、イソプレテレノール持続吸入を開始した。髄液穿刺では、初圧8 cmH_2O、細胞数3／3と髄膜炎は否定的だった。21時20分、低血糖による右眼瞼、右手の痙攣があったが、グルコース静注にて消失した。

その後、代謝性アシドーシスの進行、血中乳酸値の上昇、肝腫大が認められた。重炭酸ナトリウム持続静注、カルニチン、ジクロロ酢酸ナトリウムの投与、マンニトールの静注等によりアシドーシスの補正、脳浮腫対策、高乳酸血症対策を行ったが、多臓器不全となり、翌朝5時32分、永眠された。

	18:00	21:00	22:50	0:40	3:00
AST (IU/l)	140			530	20,400
ALT (IU/l)	48			152	7,550
LD (IU/l)	976			4,017	39,050
CK (IU/l)	273				2,672
BS (mg/dl)	258	17	44	115	128
NH3 (μg/dl)	147			145	
Na (mEq/l)	121	124		131	
K (mEq/l)	6.7	4.5		3.1	
Ca (mg/dl)	7.2	7.0			
pH	7.32	7.31	7.29	7.26	7.17
PCO2(mmHg)	28.3	19.4	23.1	24.4	20.4
BE (mmol/l)	-9.5	-16.6	-12.6	-13.4	-18.5
乳酸 (mmol/l) (正常値0.6 ~2.4 mmol/l)	2.2	4.7	7.4	9.8	13.6

図2　検査所見の推移

3　本症の臨床的特徴のまとめ

本症の臨床的特徴としては、感染症の先行、急激な発症、呼気性喘鳴、初発の痙攣、頻脈、持続する意識障害、肝腫大の進行、ALT、ASTの急速な上昇、低血糖発作、代謝性アシドーシスの進行、乳酸値の上昇等が挙げられる。

臨床診断は、急性脳症（Reye症候群）、気管支喘息、心室頻拍であった。

4　病理解剖

（1）マクロ所見

肝臓は670gと腫大し、黄白色変性、うっ血が

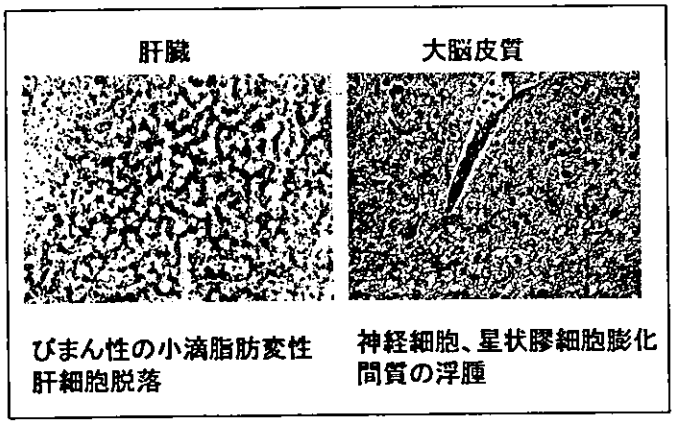

図3 病理

認められた。脳の重量は1340gと増加し、静脈怒張、脳溝狭小化が認められた。

(2) ミクロ所見

肝臓では、びまん性の小滴脂肪変性、肝細胞脱落が、大脳皮質では、神経細胞、星状膠細胞の膨化、間質の浮腫が認められ、典型的なReye症候群の所見だった。【図3】

ただし、骨髄では著しい低形成像が、脾臓ではリンパ濾胞胚中心に壊死物質が認められ、ウイルス感染または薬剤性による免疫抑制状態の可能性が示唆され、テオフィリン等の薬剤の関与も否定できなかった。

5 考察

(1) Reye症候群の原因

Reye症候群の原因としては一般的に、感染症、先天性代謝異常症、薬剤等が考えられている。

本症例では発熱を伴う喘息様気管支炎が先行し、何らかの感染症が疑われたが、ウイルス・サーベイランスでは、インフルエンザウイルス、アデノウイルス、エンテロウイルスを含めすべて陰性で、特定の感染症は判明しなかった。そこで、脂肪酸代謝異常等の先天性代謝異常症の有無、テオフィリン製剤等の薬剤の関与について考察する。

(2) Reye症候群をきたす先天性代謝異常症

有機酸代謝異常症、脂肪酸代謝異常症、尿素サイクル障害、ピルビン酸代謝障害、解糖系障害などがある。本例では、血中遊離脂肪酸分析で中鎖脂肪酸C10、極長鎖脂肪酸C14の特異的増加があり、脂肪酸代謝異常症が疑われた。中でも中鎖、極長鎖の2系統の異常があることから、多系統にわたる脱水素酵素障害が特徴であるグルタル酸尿症2型が疑われ、アシルカルニチン分析を並行して行った。結果として、遊離カルニチン、アセチルカルニチンの著増は認められたが、アシルカルニチン・プロフィールとしての病的変化は認められず、グルタル酸尿症2型と確定するには至らなかった。他の代謝性疾患について尿中有機酸・アミノ酸分析をしたが、特に異常は認められなかった。

同時に、健康な同胞に同様な分析を行ったところ、血中遊離脂肪酸検査で、極長鎖脂肪酸C14の増加が認められた。姉妹例であり、グルタル酸尿症を含め、何らかの脂肪酸代謝異常症の存在が強く疑われた。

(3)グルタル酸尿症2型について[1][2]

グルタル酸尿症2型は、ミトコンドリアの複数の脱水素反応が同時に阻害される疾患である。病因は電子伝達フラビン蛋白（EFT）のα、βサブユニット、EFT脱水素酵素（EFTQO）の欠損の3つがある。

臨床病型としては、生後まもなく死亡する新生児型と遅発型があり、遅発型の症状としては、代謝性アシドーシス、肝腫大、低血糖、高アンモニア血症などの間欠的発作を来したり、Reye症候群様症状で発症することもある。

診断は、血中遊離脂肪酸、アシルカルニチン分析で複数の炭素鎖の遊離脂肪酸、アシルカルニチンの上昇があること、急性期の尿中有機酸分析でグルタル酸の上昇があること、酵素診断などがあ

表1 グラスゴー昏睡判定表(小児用) (Hahn YS, et al. 1988)

判定基準	程度	点数
開眼	自発的に	4
	音に対して	3
	痛みに対して	2
	開眼せず	1
言語	年齢相当の発語、音に反応、固視と追視、笑み	5
	泣くがなだめられる 不穏、協調できず、周囲には関心あり	4
	不穏、泣き続ける、なだめることが困難	3
	なだめられない啼泣、周囲や両親に無関心 不眠、興奮状態	2
	発語なし	1
運動	命令に従う、自発的な動き	6
	疼痛部の位置がわかる	5
	逃避反応あり	4
	痛みに対する異常屈曲反応	3
	痛みに対する異常伸展反応	2
	動きなし	1

る。本症例では複数の炭素鎖の遊離脂肪酸の上昇を認めたが、他は正常で確定診断には至らなかった。

(4)テオフィリン関連痙攣・脳症の可能性

本症例では、来院時、心室頻拍があり、テオフィリン痙攣が疑われたが血中濃度はいわゆる治療域であった。しかし、病理所見では骨髄・脾臓の免疫抑制状態が認められ、ウイルスもしくは薬剤の関与が疑われた。我々が調べた範囲では、テオフィリンによるReye症候群の報告はなかった。しかし、テオフィリン血中濃度が治療域であっても、何らかの神経学的異常が基礎にある場合に急性脳症をきたすこともある[3][4][5]。テオフィリン関連脳症の可能性も充分考えられるが、Reye症候群様症状も同時に呈した報告は過去になく、テオフィリン関連と考えると本症例が初めての報告となる。

(5) 小児の意識障害のみかた

小児では、会話能力や知的発達の問題で、軽微な意識障害の判定が大人と同様にはできない。そこで、坂本らによる乳児用に改定された判定方法[6]や、【表1】に示すようにグラスゴーの小児用昏睡判定法[7]を参考に意識障害の程度を正確に判定する必要がある。

小児には、事故に遭遇しやすい、免疫力が弱い、恒常性を保てない、脱水症に陥りやすいなどの特徴がある。そのため、小児の意識障害の原因としては、外傷以外では、①感染症(脳炎、髄膜炎など)、②代謝異常症(低血糖、電解質異常症、Reye症候群など)、③薬物中毒(抗痙攣剤、テオフィリン製剤など)、④神経疾患(てんかん、熱性痙攣)等が成人に比して多い。その他、もやもや病、脳腫瘍、熱中症、気管支喘息大発作、急性喉頭蓋炎、不整脈、虐待なども重要である。

問診のポイントを【図4】に示す。来院状況、家族の態度などから虐待が疑われることもある。

問診のポイント

1：家族歴
- てんかん、熱性けいれんなどの神経疾患や突然死の有無

2：既往歴
- 基礎疾患
  (神経、循環器、呼吸器、内分泌・代謝、肝、腎、精神
  消化器など)
- 薬物常用の有無

3：現病歴
- 最近の外傷、感染症、予防接種の有無
- 感染症の流行状況
- 発症のしかた(突発的、急性、亜急性、再発性など)
- 前駆症状(頭痛、嘔吐、けいれん、発熱など)
- 来院状況、家族の態度

図4

治療では、①初期治療としての、気道確保、血管確保と補液、薬物投与（昇圧剤、アシドーシス・電解質・血糖補正等）などが特に重要である。並行して、②脳圧降下剤、過換気などの脳浮腫対策、③痙攣対策、④原疾患対策等を行っていく。最近、⑤脳低体温療法を積極的に行う施設もある。

6 おわりに

診断確定には至らなかったが、遊離脂肪酸分析で2系統の炭素鎖脂肪酸の上昇があり、本症例ではグルタル酸尿症を含めた脂肪酸代謝異常症が強く疑われた。今後、健康同胞に発症前の酵素診断をするべきか否か検討課題である。臨床の場面においては代謝異常の存在は推測し得ないことも多いと思われるが、小児の意識障害の場合には、後に代謝異常症の有無等を検査できるように急性期の血液、尿等の検体を保存しておく必要が高いと思われる。また、発熱、意識障害を伴う乳幼児においては、テオフィリン製剤等の使用に際し、慎重を期する必要があることをあらためて強調したい。本症例では、人工呼吸管理後も閉塞性呼吸障害が改善されず、アミノフィリン持続点滴を継続して行ったが、このことがReye症候群の病態をさらに増悪させた可能性もあり、反省すべき点であった。

参考文献

1．山口清次，日本臨床別冊先天異常症候群　辞典（上巻）：108-110,2001.

2．FrermanFE, Goodman SI: Nuclear-encoded defects of the mitochondrial chain, including glutaric acidemia type Ⅱ. In: The Metabolic Molecular Basis of Inherited Metabolic Disease 7th ed:1611-1629, McGraw-Hill, New York, 1995.

3．佐野正，岩田厚司，立木秀樹他，日本小児アレルギー学会誌11- 2: 51-57, 1997.

4．平野幸子，小児科35: 1385-1391, 1994.

5．平野幸子，兼松幸子，林北見ほか，小児アレルギー会誌 7: 227-228,1993.

6．坂本吉正，小児の意識障害、小児神経診断学，金原出版　pp33-54,1978

7．Hahn YS et al.: Impairment of consciousness and coma. In Swaiman KF et al. (eds):Pediatric Neurology Principles and Practice, 3rd ed, Mosby, St. Louis, pp861-872,1999.

nature genetics

Mutations in *EFHC1* cause juvenile myoclonic epilepsy

Toshimitsu Suzuki[1,2,12], Antonio V Delgado-Escueta[3], Kripamoy Aguan[1,12], Maria E Alonso[4], Jun Shi[1], Yuji Hara[5,6], Motohiro Nishida[5,6], Tomohiro Numata[5], Marco T Medina[3,7], Tamaki Takeuchi[1], Ryoji Morita[1], Dongsheng Bai[3], Subramaniam Ganesh[1], Yoshihisa Sugimoto[1], Johji Inazawa[2], Julia N Bailey[3,8], Adriana Ochoa[4], Aurelio Jara-Prado[4], Astrid Rasmussen[4], Jaime Ramos-Peek[4], Sergio Cordova[4], Francisco Rubio-Donnadieu[4], Yushi Inoue[9], Makiko Osawa[10], Sunao Kaneko[11], Hirokazu Oguni[10], Yasuo Mori[5,6] & Kazuhiro Yamakawa[1]

Juvenile myoclonic epilepsy (JME) is the most frequent cause of hereditary grand mal seizures[1,2]. We previously mapped and narrowed a region associated with JME on chromosome 6p12–p11 (*EJM1*)[3–5]. Here, we describe a new gene in this region, *EFHC1*, which encodes a protein with an EF-hand motif. Mutation analyses identified five missense mutations in *EFHC1* that cosegregated with epilepsy or EEG polyspike wave in affected members of six unrelated families with JME and did not occur in 382 control individuals. Overexpression of EFHC1 in mouse hippocampal primary culture neurons induced apoptosis that was significantly lowered by the mutations. Apoptosis was specifically suppressed by SNX-482, an antagonist of R-type voltage-dependent Ca^{2+} channel ($Ca_v2.3$). EFHC1 and $Ca_v2.3$ immunomaterials overlapped in mouse brain, and EFHC1 coimmunoprecipitated with the $Ca_v2.3$ C terminus. In patch-clamp analysis, EFHC1 specifically increased R-type Ca^{2+} currents that were reversed by the mutations associated with JME.

Two separate regions of the short arm of chromosome 6, 6p21.3 and 6p12–p11, are proposed to be associated with JME. In the 6p21.3-HLA region[6,7], two single-nucleotide polymorphisms (SNPs) in *BRD2* were in linkage disequilibrium with JME, although no causative coding mutations were found[8]. In contrast, families with JME from Belize, Los Angeles[3,4] and Mexico[5] showed significantly high lod scores at the 6p12–p11 locus but exclusionary lod scores at 6p21.3. An independent study of Dutch families with JME confirmed that 6p12–p11 is associated with to JME[9].

We identified 18 genes in the narrowed 3.5-cM region at 6p12–p11 (ref. 5) and excluded all of them except *EFHC1* from association with JME by mutation analyses (ref. 10 and T.S. *et al.*, unpublished data). *EFHC1* is located between the markers *D6S1960* and *D6S1024* (data not shown), spans ~72 kb and encodes a protein of 640 amino acids (**Supplementary Fig. 1** online). A domain search identified three DM10 domains, a motif with unknown function and an EF hand, a Ca^{2+} binding motif[11] (**Fig. 1a**). *EFHC1* transcripts undergo alternative splicing in exon 4, resulting in a C-terminally truncated protein (**Supplementary Fig. 1** online and **Fig. 1b**). Northern-blot analysis confirmed that both transcripts were expressed in various human tissues, including brain (**Fig. 1c**), but not in lymphocytes, as confirmed by RT-PCR (data not shown). We also identified a partial cDNA clone that corresponded to the 7-kb and 9-kb transcripts observed on northern blots. These longer transcripts could contain structures of transcript B with its extended 3′ untranslated region, as they were detected by probes 2 and 4 (**Fig. 1b,c**).

We also isolated a mouse ortholog of *EFHC1*, named *Efhc1*, and investigated its expression by RT-PCR and northern-blot analyses (**Supplementary Fig. 2** online). A 2.3-kb *Efhc1* transcript appeared on northern blots, but the analyses detected almost none of the larger transcripts that were observed in humans. We raised a polyclonal antibody to EFHC1 that recognizes amino acid residues 522–533 of both human and murine EFHC1 proteins (**Supplementary Fig. 2** online) and investigated their expression (**Fig. 1d–i**). Double-staining of mouse primary culture neurons with the antibody to EFHC1 and antibodies to MAP2 (dendrite marker) or to phosphorylated neurofilament (axon marker) showed that Efhc1 localized at soma and dendrites of neurons (**Fig. 1d–f**), but the Efhc1 signal was not observed at axons (data not shown). Immunohistochemistry of mouse brain sections showed Efhc1 signals in soma and dendrites of pyramidal neurons of the hippocampal CA1 region (**Fig. 1g**), pyramidal neurons of the cerebral cortex (**Fig. 1h**) and Purkinje cells of cerebellum (**Fig. 1i**).

We carried out mutation analyses of *EFHC1* in 44 families with JME (31 Mexican families[5], 1 family from Belize and 12 European

[1]Laboratory for Neurogenetics, RIKEN Brain Science Institute, 2-1 Hirosawa, Wako-shi, Saitama, 351-0198, Japan. [2]Department of Molecular Cytogenetics, Medical Research Institute, Tokyo Medical and Dental University, Tokyo, Japan. [3]Epilepsy Genetics/Genomics Laboratories, Comprehensive Epilepsy Program, David Geffen School of Medicine at UCLA and VA GLAHS-West Los Angeles, Room 3405 (127B), Building 500, West Los Angeles DVA Medical Center, 11301 Wilshire Boulevard, Los Angeles, California 90073, USA. [4]National Institute of Neurology and Neurosurgery, Mexico City, Mexico. [5]Center for Integrative Bioscience, The Graduate University for Advanced Studies, Okazaki, Japan. [6]Graduate School of Engineering, Kyoto University, Kyoto, Japan. [7]National Autonomous University, Tegucigalpa, Honduras. [8]Neuropsychiatric Institute, David Geffen School of Medicine at UCLA, Los Angeles, California, USA. [9]National Epilepsy Center, Shizuoka Medical Institute of Neurological Disorders, Shizuoka, Japan. [10]Department of Pediatrics, Tokyo Women's Medical University, Tokyo, Japan. [11]Department of Neuropsychiatry, School of Medicine, Hirosaki University, Aomori, Japan. [12]These authors contributed equally to this work. Correspondence should be addressed to K.Y. (yamakawa@brain.riken.go.jp) or A.V.D.E. (escueta@ucla.edu).

Published online 18 July 2004; doi:10.1038/ng1393

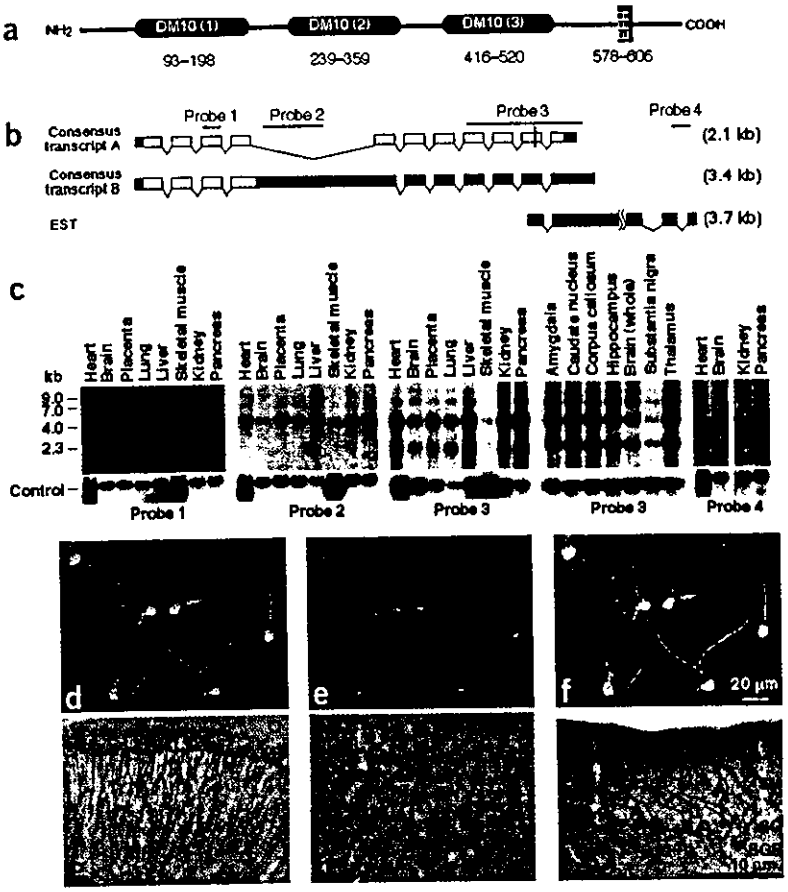

Figure 1 Structure and expression of *EFHC1*. (**a**) Schematic diagram of EFHC1 protein (encoded by transcript A). (**b**) Schematic diagrams of the *EFHC1* isoforms consensus transcript A, transcript B and an EST clone. Coding regions are shown as open boxes and presumptive untranslated regions as filled boxes. The vertical line in transcript A indicates the EF-hand domain. Relative positions of the probes used for the northern-blot analyses are shown on the top. Probe 2 is specific for transcript B. (**c**) Northern-blot analyses of *EFHC1* in human adult tissues using probes 1, 2, 3 and 4. Signals obtained for control *ACTB* (for probes 1, 2 and 4) or *GAPD* (for probe 3) probes are shown. (**d–f**) Hippocampal primary culture neurons (6 d *in vitro*) from E16 mouse embryos were double-stained with antibodies to EFHC1 (**d**) and to MAP2 (**e**). Signals of Efhc1 and MAP2 mostly overlap (**f**). (**g–i**) Sections of adult mouse brain were stained with antibody to EFHC1. (**g**) Hippocampal CA1 region. Soma and dendrites of pyramidal neurons show signals. O, stratum oriens; P, stratum pyramidal; R, stratum radiatum. (**h**) Layer III of cerebral cortex. Soma and dendrites of neurons show signals (arrows). (**i**) Cerebellum. Dendrites of Purkinje cells show intense signals (arrowheads). SG, stratum gangliosum; SGR, stratum granulosum; SM, stratum moleculare. Results of control stainings with preimmune rabbit serum or serum preabsorbed with EFHC1 peptide are shown in **Supplementary Figure 2** online.

American families[3,4]; **Fig. 2a,b**) and detected three heterozygous mutations (685T→C, 628G→A and 757G→T, resulting in the amino acid substitutions F229L, D210N and D253Y, respectively) and one double heterozygous mutation (229C→A and 662G→A, resulting in the amino acid substitutions P77T and R221H, respectively) among all 21 affected members of 6 unrelated families (**Fig. 2a**). The mutations cosegregated with disease symptoms in 13 individuals with epilepsy and 8 individuals with polyspike wave in six Mexican families with JME. Of these 13 individuals with epilepsy, 10 had JME and 3 had grand mal only. Of the 10 individuals with JME, 3 also had rare absence seizures and one had rare absence seizures in clusters. Pyknoleptic absence seizures as the only phenotype was not observed in any affected member[3]. Several family members with mutations (individual I-1 in family 1; individual II-1 in family 2; individuals II-2, II-3 and II-6 in family 4; and individual II-3 in family 5) did not have clinical epilepsy or polyspike waves, indicating that the mutations had 78% (21 of 27) penetrance[3,4]. These mutations were not observed in 382 unrelated healthy controls, implying that they are not neutral polymorphisms. Haplotype analysis suggested that there was a founder effect for a 640-kb region surrounding the double heterozygous mutations (**Fig. 2c**). Four of these mutations affected residues conserved among EFHC1 orthologs (**Supplementary Fig. 1** online). We also detected three coding (457C→T, 545G→A and 1855A→C, resulting in the amino acid substitutions R159W, R182H and I619L, respectively) and several noncoding polymorphisms in both affected and control individuals. The frequencies of these coding polymorphisms were 16% (5 of 31), 19% (6 of 31) and 10% (3 of 31), respectively, in probands of the 31 Mexican families with JME and 14% (29 of 209), 11% (23 of 213) and 5% (10 of 208), respectively, in the general population. The frequencies were higher in individuals with JME, but the differences were not statistically significant ($P = 0.78$, 0.22 and 0.38, respectively). A large three-generation family from Belize[4] carried the variant 545G→A (resulting in the amino acid substitution R182H), which cosegregated with JME in 11 affected members (**Fig. 2b**) with 65% (11 of 17) penetrance. The variant I619L segregated with JME in affected individuals of three other families. We regrouped the families into those with and without *EFHC1* mutations and recalculated lod scores separately but did not find any significant differences between scores of the two groups (data not shown).

To investigate the functional significance of EFHC1 and its mutants in neurons, we transfected mouse hippocampal primary culture neurons with enhanced green fluorescent protein (EGFP)-EFHC1 expression constructs (**Fig. 3a–i**). EFHC1-positive neurons had shorter neurites and fewer branches 16 h after transfection (**Fig. 3b**) and showed signs of neurodegeneration and cell death, including shrinkage of the cell body and fragmentation of processes 48 h after transfection (**Fig. 3d**), whereas control cultures seemed to be healthy (**Fig. 3c**). Cells transfected with *EFHC1* were TUNEL-positive, indicative of apoptosis (**Fig. 3e–g**). Next, we investigated the effects of EFHC1 mutations on cell survival by counting GFP-positive surviving cells attached to the dishes at various time points, irrespective of cellular morphologies. The cell-death effect of EFHC1 was substantially reduced by any of the five mutations associated with JME and by the double mutation 229C→A and 662G→A. In contrast, the three coding polymorphisms that were also present in the control population did not affect cell death considerably (**Fig. 3h**). Although the numbers of surviving cells transfected with mutations associated with JME seemed close to that of

vector-transfected cells, the cells transfected with mutations associated with JME had unhealthy morphology 48 h after transfection, implying that the mutations did not disrupt EFHC1 function completely. We also analyzed the effects of EFHC1 isoforms on cell survival. Transfection with a construct expressing transcript B resulted in moderate cell death, and coexpression of the wild-type transcript and transcript B had intermediate effects (**Fig. 3i**). The cellular functions of the protein encoded by transcript B are not known, but the fact that this isoform excludes the mutation 757G→T from its open reading frame suggests that this isoform may not have a large role in the pathogenesis of JME.

Because EFHC1 contains a Ca^{2+}-sensing EF-hand motif and because abnormalities of voltage-dependent Ca^{2+} channels (VDCCs) have been described in human and mouse epilepsies[12–16], we investigated whether the observed cell death is due to modulations of VDCCs. RT-PCR showed that most of the VDCC subtypes were expressed in mouse primary culture neurons, albeit at varied levels (**Fig. 3j**). Treatments of EFHC1-transfected primary culture neurons with several antagonists of VDCC subtypes indicated that SNX-482, antagonist for $Ca_v2.3$ (ref. 17), specifically increased the survival rates of EFHC1-positive neurons (**Fig. 3k** and **Supplementary Fig. 3** online).

Immunohistochemical analyses (**Fig. 4a–k**) showed that Efhc1 protein was widely expressed in adult mouse brain including hippocampus (**Fig. 4a,c**), cerebellum (**Fig. 4f**), cerebral cortex (**Fig. 4i**), thalamus, hypothalamus, amygdala and upper brainstem (data not shown) and largely overlapped with signals for $Ca_v2.3$ (ref. 18; **Fig. 4b,d,e,g,h,j,k**). Double staining of hippocampal primary culture neurons with antibodies to EFHC1 and to $Ca_v2.3$ showed signals at soma and dendrites (**Fig. 4l–n**).

Patch-clamp analyses of baby hamster kidney (BHK) cells stably expressing $Ca_v2.3$ and transiently transfected with *EFHC1* showed that EFHC1 substantially increased the R-type Ca^{2+} current generated by $Ca_v2.3$ (**Fig. 5**). Cotransfection with constructs expressing P/Q-type VDCC ($Ca_v2.1$) and EFHC1 did not increase Ca^{2+} currents (data not shown). The effects of EFHC1 on $Ca_v2.3$ were extensive and unique, even when compared with the effects of the auxiliary subunits of the Ca^{2+} channels[16,19] These results suggest that EFHC1 enhances Ca^{2+} influx through $Ca_v2.3$ and stimulates programmed cell death. Mutations associated with JME partly reversed the increase in R-type Ca^{2+} currents by EFHC1 (**Fig. 5b,c**). Incomplete reversal of EFHC1-induced Ca^{2+} influx through $Ca_v2.3$ may be responsible for the precarious state of calcium homoeostasis sensitive to the triggering effects of sleep deprivation, fatigue and alcohol in individuals with JME. The three coding polymorphisms had weaker or no reversal effects (**Fig. 5b,c**), implying that they could be functionally benign or less malignant. Transfection with the transcript B isoform moderately increased Ca^{2+} current (**Fig. 5b,c**). These results are consistent with those of the cell-death analyses (**Fig. 3h,i**).

VDCCs are often regulated by proteins that interact with the intracellular C termini of VDCCs[20]. We therefore carried out coimmunoprecipitation assays with C-terminal fragments of P/Q-type ($Ca_v2.1$),

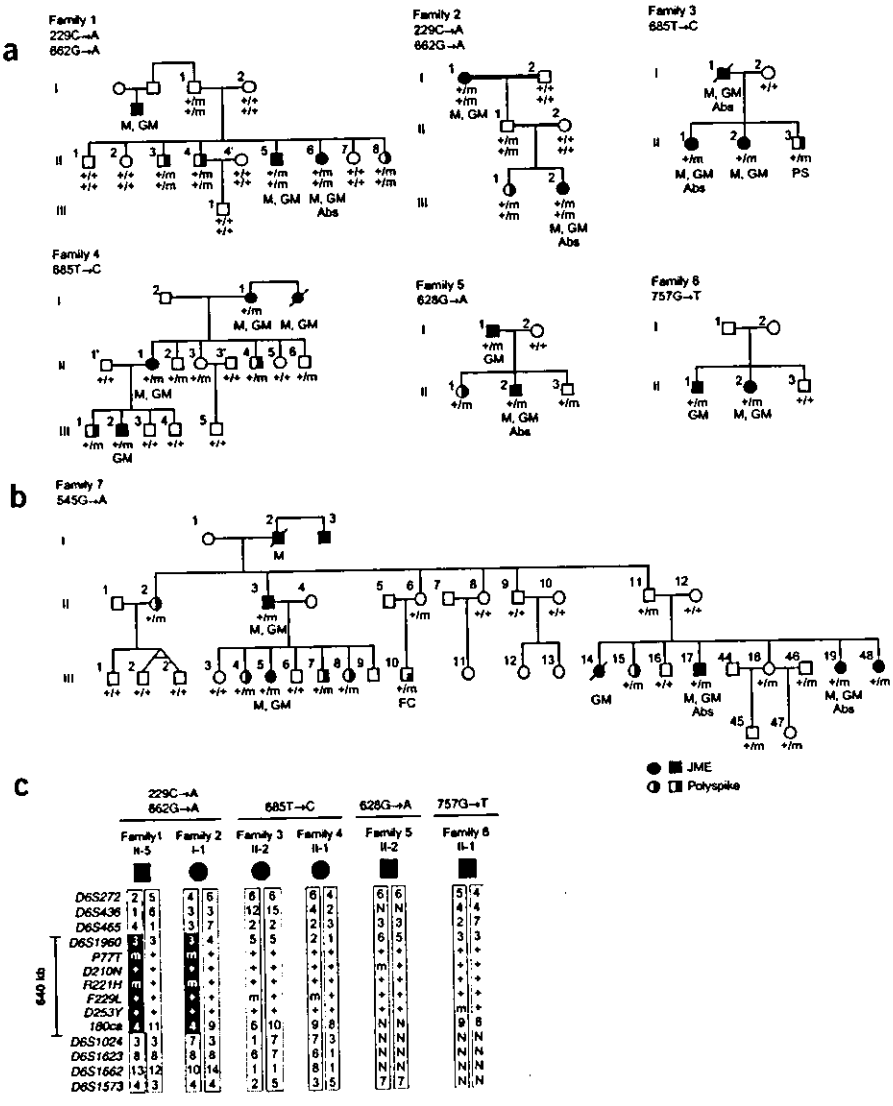

Figure 2 *EFHC1* mutations segregating with epilepsy traits in families with JME. (**a**) One double heterozygous (229C→A and 662G→A) and three heterozygous (685T→C, 628G→A, 757G→T) missense mutations cosegregated with disease symptoms in 13 individuals with epilepsy and 8 individuals with polyspike wave in six Mexican families with JME. +, wild-type allele; m, mutated allele. Filled symbols indicate individuals with JME (M, myoclonic; GM, grand-mal tonic-clonic; Abs, absence seizures; PS, photosensitivity of polyspike wave complexes); half-filled symbols indicate clinically asymptomatic family members with 3.5- to 6-Hz multispike and slow wave complexes. (**b**) The 545G→A variant segregates with JME in affected members of a large family from Belize[4] (family 7). One-quarter-filled symbol indicates an individual with febrile convulsion (FC). (**c**) Haplotypes of families with JME surrounding the *EFHC1* locus. Haplotype analysis detected identical a 640-kb series of alleles surrounding the double heterozygous mutations in apparently unrelated families 1 and 2, suggestive of a founder effect. No common alleles surrounding the mutations were found in families 3, 4, 5 and 6, suggesting that the identical mutations found in families 3 and 4 were generated by recurrent mutational events. m, mutated allele; +, wild-type allele; N, not done.

N-type ($Ca_v2.2$) and R-type ($Ca_v2.3$) VDCCs. Myc-tagged EFHC1 coprecipitated with the FLAG-tagged C terminus of $Ca_v2.3$ but not with $Ca_v2.1$ or $Ca_v2.2$ (**Fig. 6a,b**). Reciprocal coimmunoprecipitation of FLAG-tagged EFHC1 and Myc-tagged $Ca_v2.3$ C terminus also yielded positive results (**Fig. 6c,d**). Deletion analyses of EFHC1 indicated that $Ca_v2.3$ bound to the EFHC1 N terminus (amino acids 1–359), which was composed of DM10(1) and DM10(2) and contained all the mutations associated with JME (**Fig. 6c,d**). All EFHC1 mutant proteins bound to the $Ca_v2.3$ C terminus (**Supplementary Fig. 3** online).

How do mutations in EFHC1 cause JME? By compromising the apoptotic activity of EFHC1 through $Ca_v2.3$, they may prevent elimination of unwanted neurons during development of the central nervous system, lead to increased density of neurons with precarious calcium homeostases and produce hyperexcitable circuits. In fact, increased densities and dystopia of neurons have been observed in the brains of individuals with JME[21,22]. Although no seizure phenotype has been described in mice lacking $Ca_v2.3$ (ref. 23), they may have undetected minor seizure sensitivities or brain microdysgeneses. Species differences may also be a factor. Furthermore, EFHC1 protein does not bind to $Ca_v2.3$ only, but also interacts with additional number of proteins (data not shown) that may modify the JME phenotype.

We identified mutations in *EFHC1* in only 6 of 44 families with JME. Unidentified mutations may exist in intronic or regulatory regions of *EFHC1*, as was observed for Unverricht-Lundborg progressive

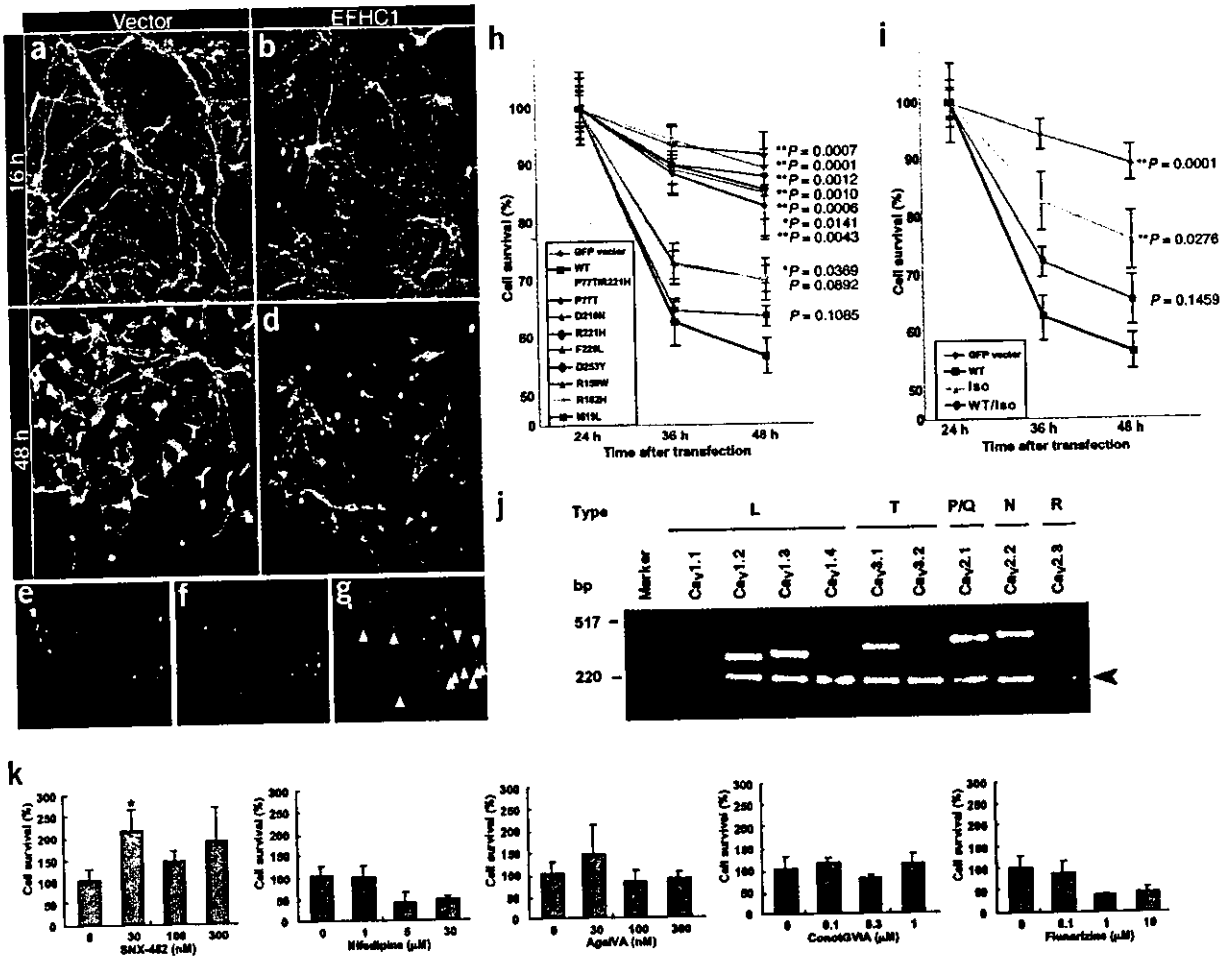

Figure 3 Activation of R-type VDCC ($Ca_v2.3$)-dependent apoptosis by EFHC1 and its reversal by mutations associated with JME. Hippocampal primary culture neurons were transiently transfected with expression constructs encoding GFP-EFHC1 (**b,d**) or with control vector encoding GFP only (**a,c**). The hippocampal neurons were stained with antibody to MAP2 (**a–d**). Cells transfected with *EFHC1* had shorter neurites and fewer branches 16 h after transfection (**b**) and neurodegeneratve morphologies, including shrinkage of the cell body and fragmentation of processes, 48 h after transfection (**d**). (**e–g**) TUNEL assay of hippocampal primary culture neurons transfected with a construct encoding Myc-EFHC1. (**e**) Staining with antibody to Myc. (**f**) TUNEL-positive cells. (**g**) Overlap of **e**, **f** and Hoechst staining of nuclear chromatin. Most of the cells transfected with EFHC1 overlap with TUNEL-positive cells (arrows). (**h,i**) Graphs of GFP-positive, surviving cell numbers 24, 36 and 48 h after transfection with constructs expressing EFHC1. Data shown are mean ± s.e.m. from seven culture wells (*t*-test in comparison with wild-type EFHC1). (**h**) Mutations associated with JME (P77T/R221H, P77T, D210N, R221H, F229L, D253Y) significantly reversed the cell-death effect of EFHC1 at 36 and 48 h after transfection, whereas the polymorphisms that occurred both in individuals affected with JME and in controls (R159W, R182H, I619L) largely maintained the cell-death effects. (**i**) GFP fusion constructs of transcript A (WT), transcript B (Iso) or GFP vector were transfected into neuron cells. Single transfection of transcript B had a moderate cell-death effect, whereas transfection with both wild-type and transcript B (half amount of DNA for each) had an intermediate effect. (**j**) Expression levels of Ca^{2+} channel α-subunits in mouse primary hippocampal neurons investigated by RT-PCR. Neuron-specific enolase was coamplified as a control (arrowhead). (**k**) Effects of VDCC antagonists on hippocampal primary culture neurons transfected with *EFHC1*. The surviving cell numbers 48 h after transfections are expressed as percentage; 100% at no antagonists. Data shown are mean ± s.e.m. ($n = 4$; control, $n = 8$). *$P < 0.05$ versus control (no antagonist; *t*-test). The results of control experiments with EGFP vectors are shown in **Supplementary Figure 3** online.

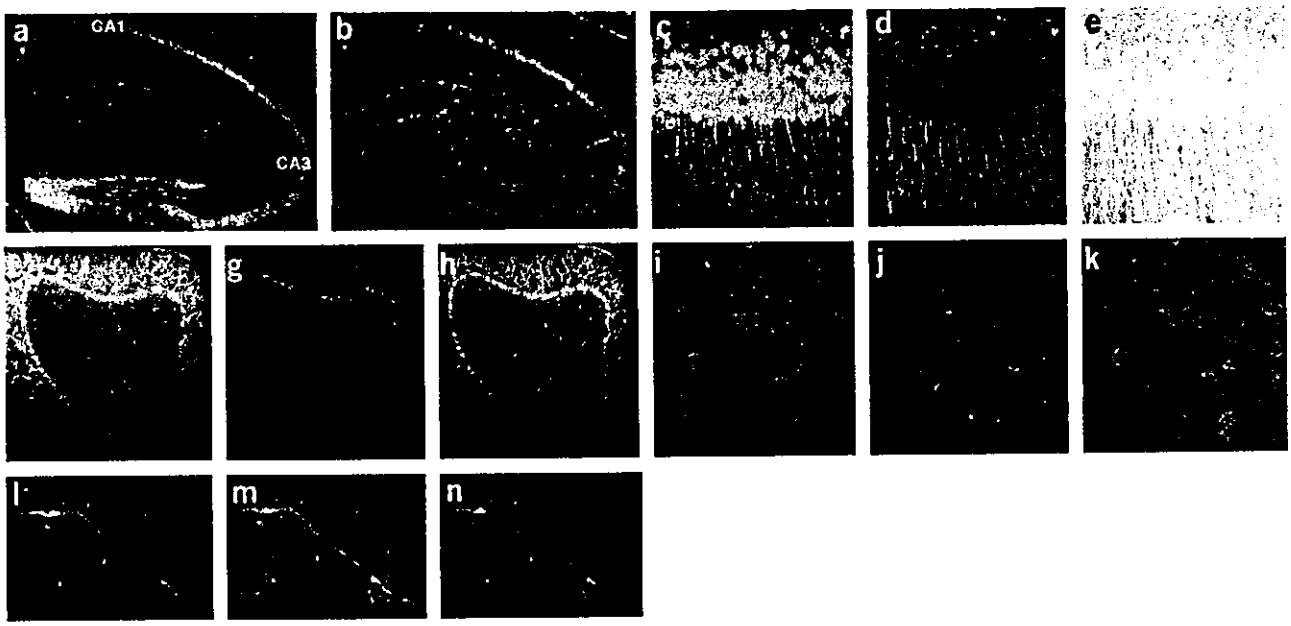

Figure 4 Colocalization of Efhc1 and $Ca_v2.3$. (**a–k**) Sections of adult mouse brain were double-stained with antiserum to EFHC1 visualized with Alexa Fluor 488 (**a**,**c**,**f**,**i**) and with antibody to $Ca_v2.3$ visualized with Alexa Fluor 594 (**b**,**d**,**g**,**j**). (**e**,**h**,**k**) Merged images. (**a**,**b**) Hippocampus. (**c–e**) Hippocampal CA1 region. (**f–h**) Cerebellum. (**i–k**) Cerebral cortex. (**l–n**) Hippocampal primary culture neurons (6 d *in vitro*) from E16 mouse embryos were double-stained with antibodies to Efhc1 (green; **l**) and to $Ca_v2.3$ (red; **m**). Signals were merged in **n**.

myoclonus epilepsy[24,25]. We searched extensively for mutations in ~100 bp of each exon-intron boundary and ~650 bp of the 5′ untranslated region of *EFHC1* in all the families with JME. Several individuals carried SNPs, but none showed significant association with the disease phenotype. The SNPs in the 5′ untranslated region also did not affect the EFHC1 promoter activity (data not shown). Further searches for mutations in expanded regions are warranted. And other genes in or outside the chromosome 6p region might be mutated in JME in some of the remaining 38 families. Common haplotypes at 6p12 in affected members of small families with JME could have occurred by chance and might not necessarily be associated with *EFHC1* mutation in all cases.

In summary, segregation of *EFHC1* mutations in individuals affected with epilepsy or polyspike wave in families with JME, together with reversal of the EFHC1-induced neuronal cell death and EFHC1-dependent increase of R-type Ca^{2+} current by mutations associated with JME, indicate that *EFHC1* is the gene on 6p12 associated with JME. Most genes incriminated as the cause of idiopathic generalized epilepsy encode ion channels. The identification of a gene that encodes a non-ion channel protein containing an EF-hand motif, which modulates and interacts with R-type VDCC and has apoptotic activity, brings a new viewpoint to the molecular pathology of idiopathic epilepsy.

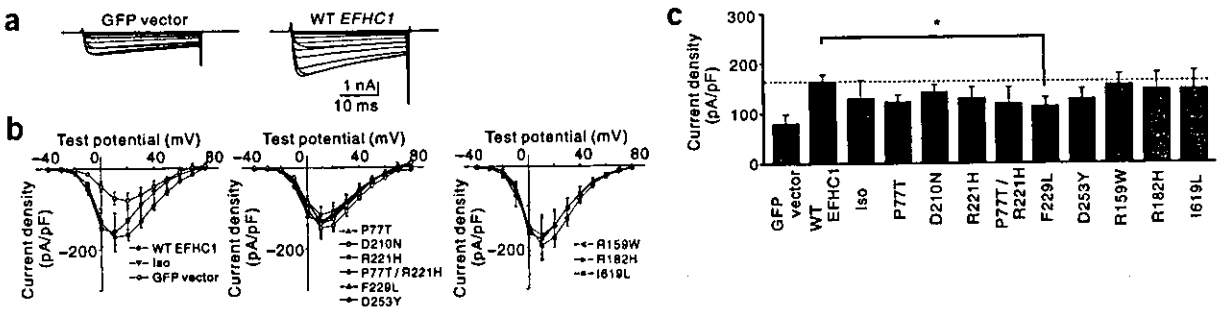

Figure 5 Potentiation of R-type VDCC ($Ca_v2.3$) activity by wild-type and its reversal by mutant EFHC1. (**a**) Ca^{2+} currents of recombinant $Ca_v2.3$ evoked in BHK cells transiently transfected with control GFP vector or wild-type (WT) *EFHC1* cDNA. Test depolarizing pulses were from –40 to 80 mV for 30 ms. Holding potential was –110 mV. (**b**) Current-voltage relationships of recombinant $Ca_v2.3$ in BHK cells transfected with GFP vector (open circles), wild-type (WT) EFHC1 (filled circles), transcript B (Iso; open downward arrowheads) and EFHC1 mutants P77T (filled triangles), D210N (open squares), R221H (filled squares), P77T and R221H (filled diamonds), F229L (open triangles), D253Y (open diamonds), R159W (open left arrowheads), R182H (filled right arrowheads), I169L (asterisks). Wild-type and mutant EFHC1 significantly upregulated R-type ($Ca_v2.3$) Ca^{2+} currents. (**c**) Ca^{2+} current densities evoked at 20mV in BHK cells coexpressing $Ca_v2.3$ in combination with EFHC1 constructs. The mutations associated with JME partly reversed the R-type current-increasing effect of EFHC1. The mutation F229L significantly suppressed the potentiation effect of EFHC1 ($^*P < 0.05$). The modulation of activation and inactivation properties of $Ca_v2.3$ by EFHC1 mutants is described in **Supplementary Table 1** online.

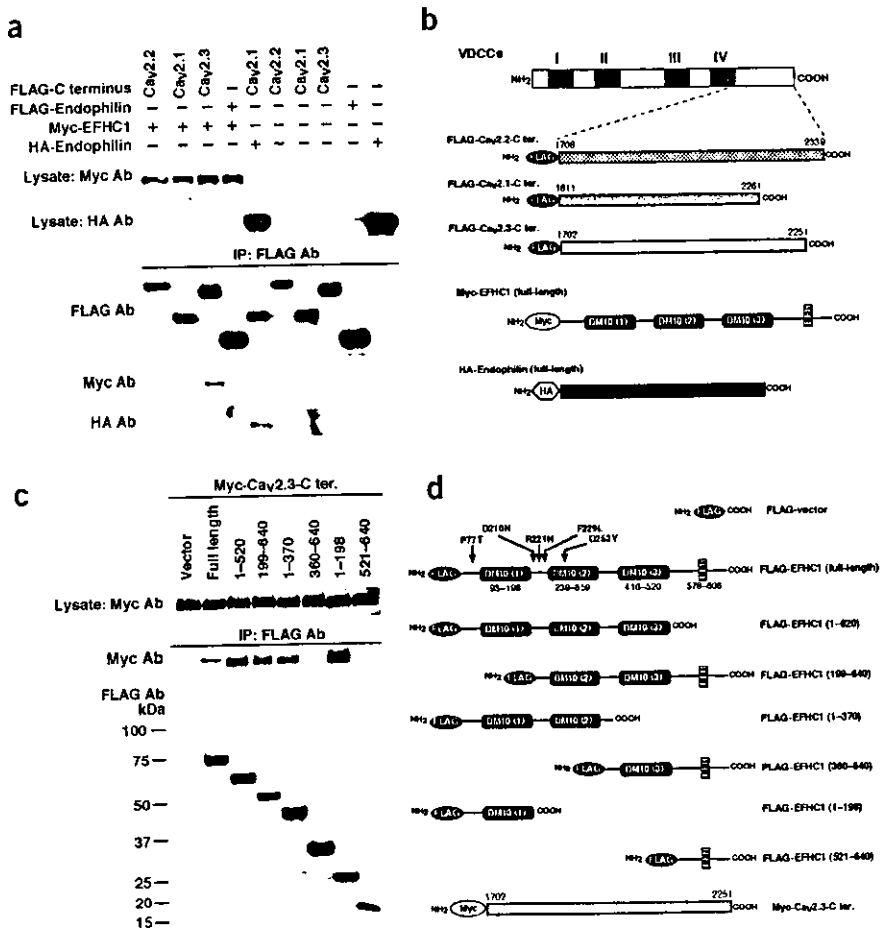

Figure 6 Immunoprecipitation assays of EFHC1 and VDCCs. (**a**) FLAG-tagged C termini of VDCCs, or FLAG-tagged endophilin, and Myc-tagged EFHC1 or hemagglutinin (HA)-tagged endophilin were coexpressed in HEK cells, and cell lysates were immunoprecipitated by antibody to FLAG. Cell lysates or immunoprecipitants were separated by electrophoresis and blotted on membranes and probed with antibodies to FLAG, to Myc or to hemagglutinin. The C termini of $Ca_v2.3$ coimmunoprecipitated with EFHC1, whereas those of $Ca_v2.1$ and $Ca_v2.2$ did not. Hemagglutinin-tagged endophilin bound to $Ca_v2.1$ C termini as reported previously[29], but FLAG-tagged endophilin did not coprecipitate with Myc-tagged EFHC1. Approximate molecular weights for EFHC1, $Ca_v2.1$, $Ca_v2.2$ and $Ca_v2.3$ C termini are 74 kDa, 52 kDa, 69 kDa and 62 kDa, respectively. (**b**,**d**) Structures of tagged proteins used for immunoprecipitation assays. The C termini of $Ca_v2.1$, $Ca_v2.2$, $Ca_v2.3$ were amplified by PCR and tagged with FLAG or Myc at their N termini. Full-length and truncated EFHC1 were amplified by PCR and tagged with Myc or FLAG at their N termini. (**c**) The assay of EFHC1 truncated proteins and C termini of $Ca_v2.3$. $Ca_v2.3$ seems to bind to the N terminus (amino acids 1–359) of EFHC1. Ab, antibody; IP, immunoprecipitation.

METHODS

Families and affected individuals. We analyzed 44 families with JME (31 Mexican families[5], 1 family from Belize and 12 European American families[3,4]). Each participating subject or responsible adult signed an informed consent form as approved by the Human Subject Protection Committee at the University of California Los Angeles School of Medicine or by the participating institutions. Criteria for inclusion of probands are as follows: (i) myoclonic seizures starting at 10–20 years of age, usually on awakening, involving shoulders, arms and other parts of the limbs (not associated with loss of consciousness); (ii) tonic-clonic or clonic tonic-clonic convulsions, usually appearing 1–2 years or, rarely, 5–10 years after the start of myoclonic seizures; (iii) normal results of neurological examination, including mental status and intelligence; and (iv) diffuse synchronous and symmetrical 3.5- to 6-Hz polyspike-wave complexes in the interictal electroencephalogram. We considered individuals with abnormal spike or polyspike wave complexes in the electroencephalogram to be affected even if they were free of seizures. The 382 unrelated healthy controls included 252 Mexicans, 96 Japanese and 34 European Americans. We extracted genomic DNA from peripheral venous blood by using QIAamp DNA Blood Mini Kit (Qiagen).

Construction of physical and transcriptional map. We constructed the physical map as described previously[26]. We used BAC and PAC sequences to search for genes registered in the National Center for Biotechnology Information BLAST database.

Domain search. We carried out a domain search in the EFHC1 amino acid sequence using the InterPro, Pfam and SMART databases.

Northern-blot analysis. We purchased Multiple Tissue Northern (MTN) blots (Clontech) for human, human brain, adult mouse and mouse whole embryo (E7–E17). We also prepared a blot using 4 μg of mouse E17 and adult whole-brain poly(A)$^+$ RNA. As probes, we amplified *EFHC1* or *Efhc1* cDNAs by PCR using human or mouse brain cDNA. We radioactively labeled the PCR products with ^{32}P using the High Prime DNA labeling kit (Roche). We hybridized membranes overnight in ExpressHyb hybridization solution (Clontech) and washed them in 0.1% saline sodium citrate and 0.1% SDS at 50 °C for 40 min. We exposed the filters to X-ray film at −80 °C overnight. We used new blots for all hybridizations.

cDNA library screening. We screened human adult brain, adult pancreas and fetal brain cDNA libraries constructed in the Lambda ZAP II vector (Stratagene) using a PCR product (probe 3; see **Fig. 1b**) as a probe according to the manufacturer's recommendations.

Generation of antibody to EFHC1. We used a synthetic peptide corresponding to amino acid residues 522–533 (QYSPEALASIQN) of human EFHC1, whose sequence is identical to that of mouse Efhc1, for immunization. We coupled the peptide, with one cysteine residue added at the N terminus, to keyhole limpet hemocyanin, mixed it with Freund's complete adjuvant in phosphate-buffered saline (PBS) and injected it into two rabbits at a dose of 1 mg protein per injection. Rabbits were boosted with peptide sequence mixed with incomplete adjuvant in PBS at 3 and 6 weeks after the first injection and bled at 8 weeks.

Primary culture of mouse hippocampal neurons. We isolated hippocampal neurons from E16 mouse embryos, plated them at $1–2 \times 10^5$ cells per well in 24-well plate containing glass coverslips coated with poly-L-lysine and grew them in serum-free NEUROBASAL medium supplemented with B27 and 0.5 mM L-glutamine (Invitrogen).

Immunocytochemistry. We fixed hippocampal primary culture neurons (6 days *in vitro*) from E16 mouse embryos with 4% paraformaldehyde in PBS

for 15 min and permeabilized them with 0.1% Triton X-100 in PBS for 5 min. We incubated the cells with blocking solution (3% normal goat serum in PBS) for 30 min and then with primary antibody in blocking solution (antibody to EFHC1 at 1:1,000 dilution; antibody to MAP-2 at 1:500 dilution (Sigma); or antibody to phosphorylated neurofilament SMI310 at 1:200 dilution (from Sternberger Monoclonals)) for 1 h at room temperature. After thoroughly washing them with PBS, we allowed the cells to react with secondary antibody (chicken antibody to rabbit IgG conjugated to Alexa Fluor 488 and donkey antibody to mouse IgG conjugated to Alexa Fluor 594; Molecular Probes) diluted at 1:1,000 for 1 h at room temperature, washed them three times in PBS and observed fluorescence with TCS SP2 microscope (Leica).

Colorimetric immunohistochemistry. We anesthetized adult ICR mice and transcardially perfused them with 4% paraformaldehyde in phosphate buffer (pH 7.4). We dissected out the brains, postfixed them for an additional 3 h at 4°C and cryoprotected them with 30% sucrose in buffer (pH 7.4). We cut 40-μm floating sections using a cryostat (Leica 1900), washed them in 0.1M PBS and immersed them in 10% normal goat serum in PBS with 0.3% Triton (PBST) for 10 min. We incubated even-numbered sections overnight in a solution of primary antibody (1:2,000 dilution for antibody to EFHC1; 1:2,000 dilution for preimmune serum; or 1:2,000 dilution for antibody to EFHC1 with 50 μg ml^{-1} EFHC1 peptide QYSPEALASIQN) diluted in 10% normal goat serum in PBST at 4 °C. After serial washes in PBST, we incubated the sections for 3 h at 40 °C with the secondary antibody, biotinylated goat antibody to rabbit IgG. We then allowed the sections to react with ABC reagent (Vectastain ABC Kit, Vector Laboratories) for 1 h at room temperature. We washed sections in Tris buffer (pH 7.2) and allowed them to react with 0.02% DAB (Doujindo) with 0.01% H_2O_2 for 20 min at room temperature. After washing them with Tris buffer and PBS, we mounted the sections on glass, dehydrated them, cleared them in xylene and placed them on coverslips.

RT-PCR. We extracted total RNA from whole brain and hippocampal primary culture neuronal cells of adult ICR mice using TRIZOL Reagent (Invitrogen) and obtained first-strand cDNA from 2 μg of total RNA using Thermoscript RNA H^- Reverse Transcriptase (Invitrogen). To amplify mouse cDNAs, we designed primers in exon 1 and exon 11 (bp 13–2,037) for *Efhc1* and for the genes encoding the Ca^{2+} channels $Ca_v1.1$, $Ca_v1.2$, $Ca_v1.3$, $Ca_v1.4$, $Ca_v3.1$, $Ca_v3.2$, $Ca_v2.1$, $Ca_v2.2$ and $Ca_v2.3$. We used neuron-specific enolase cDNA primers as controls. Primer sequences are available on request.

Mutation analysis. We screened for mutations as described previously[27]. We designed PCR primers to amplify all 11 exons of *EFHC1*, amplified genomic DNA by PCR using the Pwo DNA Polymerase (Roche) and analyzed it by heteroduplex analysis using WAVE (Transgenomic) and direct-sequencing using ABI auto-sequencer type 3700 (PE Applied Biosystems). Primer sequences are available on request.

Expression constructs and mutagenesis. We amplified the complete open reading frame of *EFHC1* (transcript A) from human adult brain cDNA (Clontech) by PCR using *Pyrobest* (TaKaRa) and cloned it into pEGFPC2 (Clontech), pcDNA3-MycN (Invitrogen) or pcDNA3-FlagN (Invitrogen) vectors. We also amplified the sequence encoding transcript B from human adult brain cDNA by PCR and cloned it into pEGFPC2. We fused the GFP, Myc or FLAG tag sequences at the N terminus of EFHC1. We introduced mutations by using the Quick Change site-directed mutagenesis kit (Stratagene) and confirmed the nucleotide changes as well as the integrity of the full sequences by DNA sequencing.

Transfection and immunostaining of mouse hippocampal neurons. On day 4, we transfected mouse hippocampal neurons with constructs encoding wild-type and mutant EFHC1 proteins using LIPOFECTAMINE2000 (Invitrogen). We fixed cultures with 4% paraformaldehyde in PBS 16 and 48 h after transfection, permeabilized them with 0.3% Triton X-100, blocked them in 3% normal goat serum in PBS and treated them with mouse monoclonal antibody to MAP-2 (1:500; Sigma) and goat antibody to mouse IgG conjugated with Alexa Fluor 594 (1:1,000; Molecular Probes).

TUNEL assay. We transfected neurons with a construct encoding wild-type EFHC1 (pcDNA-MycN-EFHC1-WT) on day 4 using LIPOFECTAMINE2000 and detected neuronal apoptosis 48 h later using the DeadEnd Fluorometric TUNEL System (Promega). We visualized nuclei with Hoescht 33342 (Molecular Probes). We also stained the cells with antibody to Myc (1:200; Cell Signaling) and goat antibody to rabbit IgG conjugated to Alexa Fluor 594 (1:1,000). All experiments were carried out in duplicate wells and repeated at least three times. We observed neurons using a confocal microscope (Olympus Fluoview) 48 h after transfection.

Cell-death analyses with EFHC1 mutants. We transfected hippocampal primary culture neurons with constructs expressing GFP-tagged wild-type EFHC1, EFHC1 carrying mutations associated with JME EFHC1 carrying polymorphisms or EFHC1 transcript B or with GFP vector alone on day 4 using LIPOFECTAMINE2000. We counted surviving cells as GFP-positive cells that attached to dishes. At each counting, we carefully removed detached (dead) cells by changing the culture medium. We did not consider cell morphology (shape, length and number of neurites, shrinkage, etc.) in the counting. We counted surviving cells 24, 36 and 48 h after transfection. We repeated the analyses twice using two independently prepared expression constructs. We counted neurons in seven wells of 24-well plates for each transfection and time point. Experiments were done in a blinded fashion.

Cell-death analyses with VDCC inhibitors. We transfected mouse hippocampal primary culture neurons with pEGFP-EFHC1 construct on day 6 *in vitro* with antagonists and fixed them 48 h after transfection. We added Ca^{2+} channel inhibitors, ω-Agatoxin IVA (Peptide Institute) for P/Q-type ($Ca_v2.1$), ω-Conotoxin GVIA (Peptide Institute) for N-type ($Ca_v2.2$), SNX-482 (Peptide Institute) for R-type ($Ca_v2.3$), flunarizine (Nacalai Tesque) for T-type and nifedipine (Sigma) for L-type VDCCs, directly to neuronal cultures 3 h after transfection.

Fluorescence immunohistochemistry. We perfused and fixed adult ICR mice as described above. We transferred the brain samples to molds containing Tissue-Tek OCT medium and froze them with CO_2 air. We prepared floating frozen sections (20 μm) by cryostat. We rinsed sections in PBS, blocked them with 5% fetal bovine serum in PBS with 0.3% Triton X-100 for 1 h at room temperature and then incubated them for 72 h at 4 °C with the rabbit polyclonal antibody to EFHC1 diluted at 1:3,000 and then with goat polyclonal antibody to α1E ($Ca_v2.3$, C-20; Santa Cruz Biotechnology) diluted at 1:10. We incubated the sections with the secondary antibodies (chicken antibody to rabbit IgG conjugated to Alexa Fluor 488 and donkey antibody to goat IgG conjugated to Alexa Fluor 564; Molecular Probes) diluted at 1:300 for 1 h at room temperature. Images were acquired under a TCS SP2 microscope (Leica).

Electrophysiological analysis. We cultured a BHK cell line (BII-104-2) stably transfected with the α_{1E} (BII), α_2/δ and β_{1a} subunits[28] in Dulbecco's modified Eagle medium containing 10% fetal bovine serum, 30 U ml^{-1} penicillin and 30 mg ml^{-1} streptomycin. To transiently express wild-type or mutant EFHC1, we transfected BHK (BII-104-2) cells with the pEGFP-C2 plasmids (Clontech) containing enhanced GFP (EGFP) fused with cDNA encoding wild-type or mutant EFHC1 using SuperFect Transfection Reagent (Qiagen). For control experiments, we transiently expressed EGFP by transfecting BHK (BII-104-2) cells with the same amount of pEGFP without the EFHC1 inserts. We treated cells with trypsin, diluted them into Dulbecco's modified Eagle medium and plated them onto glass coverslips 18 h after transfection. We recorded Ca^{2+} currents 24–48 h after transfection from GFP-positive cells. We recorded currents from BHK (BII-104-2) cells at room temperature (22–25 °C) using patch-clamp techniques of whole-cell mode with an EPC-9 amplifier (HEKA, Germany). We made patch pipettes from borosilicate glass capillaries (1.5 mm outer diameter and 0.87 mm inner diameter; Hilgenberg) by using a model P-97 Flaming-Brown micropipette puller (Sutter Instrument). Pipette resistance ranged from 2 to 3 MW when filled with the pipette solutions described below. The series resistance was electronically compensated to >70%, and both the leakage and the remaining capacitance were subtracted by –P/6 method. We sampled currents at 100 kHz in activation kinetics, and otherwise sampled them at 50 kHz and filtered them at 10 kHz. We recorded Ca^{2+} currents in an external solution that contained 3 mM $CaCl_2$,

148 mM tetraethylammonium chloride, 10 mM glucose and 10 mM HEPES buffer (pH adjusted to 7.4 with Tris-OH). The pipette solution contained 85 mM Cs-aspartate, 40 mM CsCl, 4 mM $MgCl_2$, 5 mM EGTA, 2 mM ATP2Na, 5 mM HEPES buffer and 8 mM creatine-phosphate (pH adjusted to 7.4 with CsOH). To determine the voltage dependence of activation, we normalized the amplitude of tail currents at −50 mV after 5-ms test pulse (−40 to 90 mV) to the maximal tail current amplitude. To determine the voltage dependence of inactivation, we normalized the amplitude of currents elicited by the 20-ms test pulse to 30 mV after 10 ms of repolarization to −110 mV following 2 s of displacement of holding potentials (−110 mV to 20 mV) to the current amplitude elicited by the test pulse after the 2-s holding potential displacement to −110 mV. All values are given as mean ± s.e. Statistical comparison was done by Student's *t*-test. The experiments were done in a blinded fashion.

Immunoprecipitation. We collected HEK cells 20 h after transfection with EFHC1 expression constructs. We washed the cells in PBS, scraped them and homogenized them in the lysis buffer (10 mM Tris (pH 8.0), 150 mM NaCl and 5mM EDTA) supplemented with protease inhibitors (Complete; Roche). We removed cellular debris by centrifugation at 12,000*g* for 10 min at 4 °C. We precleared the supernatants with protein G–Sepharose (Amersham Pharmacia Biotech) for 2 h at 4 °C and then incubated them with monoclonal antibody to FLAG M2 Affinity Gel (Sigma) or antibody to Myc (Santa Cruz Biotechnology) for 12 h at 4 °C. We used protein G–Sepharose for precipitation with antibody to Myc. We washed the beads with lysis buffer five times and then eluted them with either FLAG peptide or SDS sample buffer for immunoblot analyses.

Western-blot analysis. We placed confluent HEK cells transiently transfected with EFHC1 expression constructs on ice and washed them twice with ice-cold PBS. We scraped cells from the dishes and homogenized them in a hypotonic buffer (0.25 M sucrose, 10 mM Tris-HCl, 10 mM NaCl and 1 mM EDTA (pH 7.5)) supplemented with protease inhibitors (Complete; Roche). We centrifuged the lysate at 3,300*g* for 5 min to remove nuclei and used the supernatant as total cytosolic protein. We separated the samples on a 4–20% gradient SDS-polyacrylamide gel and transferred them onto a nitrocellulose filter (0.45 μm; Schleicher & Schuell) using an electroblot apparatus (Bio-Rad) at 100 V for 1 h in transfer buffer (25 mM Tris-HCl, 192 mM glycine, 0.1% SDS and 20% (v/v) methanol). We incubated the filter in blocking solution (50 mM Tris-HCl, 200 mM NaCl and 1 mM $MgCl_2$ (pH 7.4)) containing 3.5–10% nonfat dry milk powder at 37 °C for 1 h. The membrane was processed through sequential incubations with primary antibody (antibody to EFHC1 at 1:1,000 dilution; mouse monoclonal antibody to GFP (Roche) at 1:1,000 dilution; rabbit polyclonal antibody to Myc (Cell Signaling) at 1:1,000 dilution; goat antibody to hemagglutinin (Roche) at 1:1,000 dilution; or antibody to FLAG conjugated to horseradish peroxidase (Sigma) at 1:1,000 dilution) for 1 h and then with 0.4 μg ml^{-1} secondary antibody conjugated to horseradish peroxidase (Santa Cruz Biotechnology). We visualized immunoreactive proteins on the filter using the Western Lighting Chemiluminescence Reagent Plus (Perkin Elmer Life Sciences).

URLs. The National Center for Biotechnology Information BLAST database is available at http://www.ncbi.nlm.nih.gov/BLAST/. The InterPro, Pfam and SMART databases are available at http://www.ebi.ac.uk/InterProScan/, http://pfam.wustl.edu/hmmsearch.shtml and http://smart.embl-heidelberg.de/, respectively.

Accession numbers. GenBank: *EFHC1* transcript A, AK001328; *EFHC1* transcript B, AL122084; *EFHC1* EST clone, AY608689; mouse *Efhc1* ortholog, AK006489; pig EST clone, AW344780; cow EST clones, BE666117 and AV595456. SNP database: 475C→T (R159W), rs3804506; 545G→A (R182H), rs3804505.

Note: Supplementary information is available on the Nature Genetics website.

ACKNOWLEDGMENTS
We thank the family members for participating in this study; Y. Itsukaichi, K. Yamada, Y. Tsutsumi, K. Shoda, E. Mazaki, A. Nitta, N. Okamura, C. Uchikawa, M. Hishinuma and S.G. Pietsch for their help; and the Research Resources Center of RIKEN Brain Science Institute for DNA sequencing analysis and generation of rabbit polyclonal antibodies. This work was supported in part by a grant from RIKEN Brain Science Institute, Japan. A.V.D.E. is partly supported by a grant from the US National Institutes of Health.

COMPETING INTERESTS STATEMENT
The authors declare that they have no competing financial interests.

Received 4 March; accepted 21 May 2004
Published online at http://www.nature.com/naturegenetics/

1. Janz, D.C.W. Impusive-petit mal. *J. Neurol.* **176**, 344–386 (1957).
2. Delgado-Escueta, A.V. *et al.* Mapping and positional cloning of common idiopathic generalized epilepsies: juvenile myoclonus epilepsy and childhood absence epilepsy. *Adv. Neurol.* **79**, 351–374 (1999).
3. Liu, A.W. *et al.* Juvenile myoclonic epilepsy locus in chromosome 6p21.2-p11: linkage to convulsions and electroencephalography trait. *Am. J. Hum. Genet.* **57**, 368–381 (1995).
4. Liu, A.W. *et al.* Juvenile myoclonic epilepsy in chromosome 6p12-p11: locus heterogeneity and recombinations. *Am. J. Med. Genet.* **63**, 438–446 (1996).
5. Bai, D. *et al.* Juvenile myoclonic epilepsy: Linkage to chromosome 6p12 in Mexico families. *Am. J. Med. Genet.* **113**, 268–274 (2002).
6. Sander, T. *et al.* Refined mapping of the epilepsy susceptibility locus EJM1 on chromosome 6. *Neurology* **49**, 842–847 (1997).
7. Greenberg, D.A. *et al.* Reproducibility and complications in gene searches: linkage on chromosome 6, heterogeneity, association, and maternal inheritance in juvenile myoclonic epilepsy. *Am. J. Hum. Genet.* **66**, 508–516 (2000).
8. Pal, D.K. *et al.* BRD2 (RING3) is a probable major susceptibility gene for common juvenile myoclonic epilepsy. *Am. J. Hum. Genet.* **73**, 261–270 (2003).
9. Pinto, D. *et al.* Evidence for linkage between juvenile myoclonic epilepsy-related idiopathic generalized epilepsy and 6p11-12 in Dutch families. *Epilepsia* **45**, 211–217 (2004).
10. Suzuki, T. *et al.* Identification and mutational analysis of candidate genes for juvenile myoclonic epilepsy on 6p11-p12: LRRC1, GCLC, KIAA0057 and CLIC5. *Epilepsy Res.* **50**, 265–275 (2002).
11. Braunewell, K.H. & Gundelfinger, E.D. Intracellular neuronal calcium sensor proteins: a family of EF-hand calcium-binding proteins in search of a function. *Cell Tissue Res.* **295**, 1–12 (1999).
12. Escayg, A. *et al.* Coding and noncoding variation of the human calcium-channel beta 4-subunit gene CACNB4 in patients with idiopathic generalized epilepsy and episodic ataxia. *Am. J. Hum. Genet.* **66**, 1531–1539 (2000).
13. Jouvenceau, A. *et al.* Human epilepsy associated with dysfunction of the brain P/Q-type calcium channel. *Lancet* **358**, 801–807 (2001).
14. Fletcher, C.F. *et al.* Absence epilepsy in tottering mutant mice is associated with calcium channel defects. *Cell* **87**, 607–617 (1996).
15. Burgess, D.L., Jones, J.M., Meisler, M.H. & Noebels, J.L. Mutation of the Ca^{2+} channel beta subunit gene Cchb4 is associated with ataxia and seizures in the lethargic (lh) mouse. *Cell* **88**, 385–392 (1997).
16. Letts, V.A. *et al.* The mouse stargazer gene encodes a neuronal Ca^{2+}-channel gamma subunit. *Nat. Genet.* **19**, 340–347 (1998).
17. Newcomb, R. *et al.* Selective peptide antagonist of the class E calcium channel from the venom of the tarantula Hysterocrates gigas. *Biochemistry* **37**, 15353–15362 (1998).
18. Yokoyama, C.T. *et al.* Biochemical properties and subcellular distribution of the neuronal class E calcium channel alpha 1 subunit. *J. Neurosci.* **15**, 6419–6432 (1995)
19. Wakamori, M. *et al.* Single tottering mutations responsible for the neuropathic phenotype of the P-type calcium channel. *J. Biol. Chem.* **273**, 34857–34867 (1998).
20. Catterall, W.A. Structure and regulation of voltage-gated Ca^{2+} channels. *Annu. Rev. Cell Dev. Biol.* **16**, 521–555 (2000).
21. Woermann, F.G., Sisosiya, S.M., Free, S.L. & Duncan, J.S. Quantitative MRI in patients with idiopathic generalized epilepsy - Evidence of widespread cerebral structural changes. *Brain* **121**, 1661–1667 (1998).
22. Meencke, H.J. & Veith,G. The relevance of slight migrational disturbances (microdysgenesis) to the etiology of the epilepsies. in *Jasper's Basic Mechanisms of the Epilepsies, 3rd Edition, Advances in Neurology* vol. 79 (eds. Delgado-Escueta, A.V., Wilson, W.A., Olsen, R.W. and Porter, R.J.) 123–131 (Lippincott Williams and Wilkins, Philadelphia, 1999).
23. Saegusa, H. *et al.* Altered responses in mice lacking α_{1E} subunit of the voltage-dependent Ca^{2+} channel. *Proc. Natl. Acad. Sci. USA* **97**, 6132–6137 (2000).
24. Pennacchio, L.A. *et al.* Mutations in the gene encoding cystatin B in progressive myoclonus epilepsy (EPM1). *Science* **271**, 1731–1734 (1996).
25. Virtaneva, K. *et al.* Unstable minisatellite expansion causing recessively inherited myoclonus epilepsy, EPM1. *Nat. Genet.* **15**, 393–396 (1997).
26. Sugimoto, Y. *et al.* Childhood absence epilepsy in 8q24: refinement of candidate region and construction of physical map. *Genomics* **68**, 264–272 (2000).
27. Morita, R. *et al.* Exclusion of the JRK/JH8 gene as a candidate for human childhood absence epilepsy mapped on 8q24. *Epilepsy Res.* **37**, 151–158 (1999).
28. Niidome, T., Kim, M.S., Friedrich, T. & Mori, Y. Molecular cloning and characterization of a novel calcium channel from rabbit brain. *FEBS Lett.* **308**, 7–13 (1992).
29. Chen, Y. *et al.* Formation of an endophilin-Ca^{2+} channel complex is critical for clathrin-mediated synaptic vesicle endocytosis. *Cell* **115**, 37–48 (2003).